Journal of the American Heart Association

ORIGINAL RESEARCH

Integrated Multilayer Omics Reveals the Genomic, Proteomic, and Metabolic Influences of Histidyl Dipeptides on the Heart

Keqiang Yan, PhD*; Zhanlong Mei, PhD*; Jingjing Zhao, PhD*; Md Aminul Islam Prodhan, PhD; Detlef Obal, MD, PhD; Kartik Katragadda, MD; Benjamin Doelling, BS; David Hoetker, BS; Dheeraj Kumar Posa, MD; Liqing He, PhD; Xinmin Yin, PhD; Jasmit Shah, PhD; Jianmin Pan, PhD; Shesh Rai, PhD; Pawel Konrad Lorkiewicz, PhD; Xiang Zhang, PhD; Siqi Liu, PhD; Aruni Bhatnagar, PhD; Shahid P. Baba, PhD

BACKGROUND: Histidyl dipeptides such as carnosine are present in a micromolar to millimolar range in mammalian hearts. These dipeptides facilitate glycolysis by proton buffering. They form conjugates with reactive aldehydes, such as acrolein, and attenuate myocardial ischemia–reperfusion injury. Although these dipeptides exhibit multifunctional properties, a composite understanding of their role in the myocardium is lacking.

METHODS AND RESULTS: To identify histidyl dipeptide–mediated responses in the heart, we used an integrated triomics approach, which involved genome-wide RNA sequencing, global proteomics, and unbiased metabolomics to identify the effects of cardiospecific transgenic overexpression of the carnosine synthesizing enzyme, carnosine synthase (Carns), in mice. Our result showed that higher myocardial levels of histidyl dipeptides were associated with extensive changes in the levels of several microRNAs, which target the expression of contractile proteins, β-fatty acid oxidation, and citric acid cycle (TCA) enzymes. Global proteomic analysis showed enrichment in the expression of contractile proteins, enzymes of β-fatty acid oxidation, and the TCA in the Carns transgenic heart. Under aerobic conditions, the Carns transgenic hearts had lower levels of short- and long-chain fatty acids as well as the TCA intermediate—succinic acid; whereas, under ischemic conditions, the accumulation of fatty acids and TCA intermediates was significantly attenuated. Integration of multiple data sets suggested that β-fatty acid oxidation and TCA pathways exhibit correlative changes in the Carns transgenic hearts at all 3 levels.

CONCLUSIONS: Taken together, these findings reveal a central role of histidyl dipeptides in coordinated regulation of myocardial structure, function, and energetics.

Key Words: genomics ■ heart ■ histidyl dipeptides ■ metabolomics ■ proteomics ■ transcriptomics ■ triomics

Glycolytically active tissues—heart, skeletal muscle, and brain––contain small-molecular-weight histidyl dipeptides (227–241 Da), such as carnosine (β-alanine-histidine) and anserine (β-alanine-N^{π}-histidine). These dipeptides are present at micromolar to millimolar levels in the myocardium and are synthesized by the ligation of a nonproteogenic amino acid, β-alanine with histidine, via the enzyme carnosine synthase (Carns).[1,2] Because the pKa value of histidyl dipeptides is close to the physiological pH

Correspondence to: Shahid P. Baba, PhD, Department of Medicine, Diabetes and Obesity Center, CLB Enviro me Institute, 580 South Preston Street, Delia Baxter Building, Room 304A, University of Louisville, Louisville, KY 40202. Email: spbaba01@louisville.edu

*K. Yan, Z. Mei, and J. Zhao contributed equally.

Supplemental Material is available at https://www.ahajournals.org/doi/suppl/10.1161/JAHA.121.023868

For Sources of Funding and Disclosures, see page 18.

JAHA is available at: www.ahajournals.org/journal/jaha

CLINICAL PERSPECTIVE

What Is New?

- Our findings suggest that histidyl dipeptides exert influence on heart function by affecting the cardiac transcriptome, proteome, and metabolome.
- Increasing histidyl dipeptides by transgenic overexpression in the mouse heart improves fatty acid and glucose utilization during ischemia.
- Succinate, a universal marker of ischemic injury that causes oxidative stress, is decreased, and fumarate, which imparts protection from ischemic injury, is increased by histidyl dipeptide overexpression in the heart.

What Are the Clinical Implications?

- Histidyl dipeptides levels affect multiple mechanisms causing ischemic injury; therefore, enhancing their levels in the heart could serve as a novel strategy to provide cardioprotection.

Nonstandard Abbreviations and Acronyms

Carns	carnosine synthase
CarnsTg	carnosine synthase transgenic
CPT	carnitine palmitoyltransferase
DEG	differentially expressed gene
DEP	differentially expressed protein
FA	fatty acid
FFA	free fatty acid
GC	gas chromatography
GO	gene ontology
KEGG	Kyoto Encyclopedia of genes and genomes
MHC	myosin heavy chain
MS	mass spectrometry
MSTFA	N-methyl-N-yert-butyldimethylsilyltrifluro acetamide
MTBSTFA	N-trimethylsilyl-N-methyl trifluroacetamide
MYL	myosin light chain
PLS-DA	partial least squares discriminant analysis
PPAR	peroxisome proliferator-activated receptor
TCA	citric acid cycle

(pKa 6.8–7.1), these dipeptides exhibit high buffering capacity. As a result, they buffer intracellular pH and facilitate glycolysis during periods of vigorous physical activity and tissue ischemia.[2,3] In addition to their high buffering capacity, histidyl dipeptides are also efficient quenchers of reactive oxygen species, as well as lipid peroxidation products, such as reactive carbonyls 4 hydroxy-2-trans-nonenal. They also chelate first transition metals.[4–7] In addition to their direct participation in regulating metabolism, these peptides can also affect long-term metabolic capacity and energy utilization. Previous work has shown that histidyl dipeptides increase the expression of several metabolic enzymes, such as pyruvate dehydrogenase 4.[8,9] They can also alter the release of microRNAs (miRNAs)[10] and influence several signaling pathways, such as those that involve the hypoxia-inducible factor α,[11] AKT/mTOR,[12] and STAT.[13] In addition, β-alanine, which is a rate-limiting precursor in the synthesis of histidyl dipeptides,[14] increases the expression of transcription factors, such as peroxisome proliferator-activated receptor (PPAR) δ.[15] Although histidyl dipeptides are synthesized from endogenous amino acids by Carns, the levels of these dipeptides in the heart and skeletal muscle can also be increased by dietary intake of β-alanine or by increasing physical activity. In contrast the levels of these peptides are suppressed in dysfunctional tissues such as the failing heart.[14,16] Nevertheless, despite this evidence linking histidyl dipeptides to multiple cellular and metabolic processes, and changes in histidyl dipeptide levels to several physiological and pathological conditions, an integrated understanding of their influence on the genes, proteins, and metabolites remains elusive.

Prior work has shown that perfusion with carnosine improves postischemic contractile function in mouse or rat hearts.[5,17] Likewise, it has been reported that carnosine supplementation increases myocardial levels of carnosine and imparts protection against ischemia–reperfusion injury.[18] Recently, we generated a cardiospecific Carns transgenic (CarnsTg) mice,[18] in which there was a significant elevation in the myocardial levels of histidyl dipeptides. Studying these mice provided, for the first time, an opportunity to understand the effects of elevated myocardial histidyl dipeptides, independent of changes in physical activity and/or nutrition. As previously reported, we found that CarnsTg mice exhibit normal cardiac function, and that an increase in the myocardial synthesis of histidyl dipeptides enhances intracellular pH buffering, facilitates glucose utilization, and attenuates myocardial ischemia–reperfusion injury.[18] However, despite this evidence, an in-depth understanding of the metabolic pathways affected by these dipeptides in the heart is lacking. Thus, to dissect the effect of these dipeptides, we performed genome-wide RNA sequencing (RNA-seq), global proteomics, and untargeted metabolomics of the CarnsTg hearts, and integrated the three data sets to characterize the interactions at the gene, protein, and metabolic levels. In addition, we performed

untargeted metabolomic analysis of the CarnsTg heart after short durations of ischemia to examine the effects of these dipeptides on cardiac fuel utilization in the ischemic heart. These results represent a unique systems-level approach that combines transcriptomic, proteomic, and metabolomic data sets to generate new insights into the potential mechanisms by which histidyl peptides regulate cardiac metabolism and function and modify cardiac ischemic injury.

METHODS

The data that support the findings of this study are available from the corresponding author on reasonable request.

Animals

Adult male wild-type (WT) C57 and cardiospecific α–myosin heavy chain (MHC)-CarnsTg mice were used for metabolomics, transcriptomics, and proteomics. All experimental procedures were conducted using protocols reviewed and approved by the Institutional Animal Care and Use Committee at University of Louisville.

RNA Extraction and RNA-Seq

Total RNA was extracted from WT and CarnsTg mice heart tissues using TRIzol reagent (Invitrogen, Thermo Fisher Scientific, Waltham, MA, USA) and RNeasy Mini Kit (QIAGEN). The RNA samples with A260/A280 >1.8, A260/A230 >1.8, and RNA integrity number >8 were considered acceptable for library construction. Library preparation and sequencing were conducted according to standard procedures at Beijing Genomics Institute (Shenzhen, China). Briefly, the messenger RNAs were enriched with oligo (dT) magnetic beads followed by complementary DNA synthesis with random hexamer-primer, end repair, adenine addition, and adaptor ligation. The ligation products were amplified with polymerase chain reaction and their quality was carefully evaluated. The standard barcoded RNA-seq libraries were generated and RNA sequences were measured by Illumina HiSeq 4000 (Illumina) according to the manufacturer's instructions. The resulting reads were mapped against the mice (*Mus musculus*) reference genome using Bowtie2 and HISAT to treat clean reads and using RSEM software to quantify transcripts. The transcript quantification was estimated in units of fragments per kilobase of transcript per million mapped reads [$10^6C/(NL/10^3)$], where C is the number of fragments matched to the specific gene, N is the number of the fragments matched to the reference genome, and L is the bases of the specific gene. Transcriptomic data are available at https://ncbi.nlm.nih.gov/geo, ID:GSE192583.

Protein Extraction

The frozen hearts from the WT and CarnsTg mice were homogenized in Tris buffer (25 mmol/L Tris–HCl, pH 7.4, 0.5 mmol/L EDTA, 0.5 mmol/L EGTA, 1 mmol/L PMSF, 1 mmol/L DTT, 25 μg/mL leupeptin, 25 mmol/L NaF, and 1 mmol/L Na_3VO_4), followed by sonication and centrifugation at 14 000*g* for 15 minutes. The supernatants were collected and protein concentration was measured by Bradford assay. Proteins in the supernatants were reduced with 10 mmol/L DTT at 56 °C for 60 minutes and alkylated with 55 mmol/L iodoacetamide at room temperature for 45 minutes. The treated supernatant was mixed with trypsin at a ratio of 60:1 and the tryptic digestion was performed at 37 °C for 12 hours. The digested products were centrifuged at 10 000*g* to remove debris and the resulting supernatant was ready for peptide analysis.

Quantitative Proteomics Based On Data-Independent Acquisition

Equal amounts of digested peptides from each heart sample were taken for analysis of quantitative proteomics. The peptides were chromatographically separated using an Ekspert NanoLC 415 single gradient system (Eksigent Technologies) coupled with a C18 column (50 cm×75 μm, Dionex). The mobile phases consisted of solvent A (0.1% formic acid in 5% acetonitrile water) and solvent B (0.1% formic acid in 95% acetonitrile). The step gradient was run at 300 nL/min, starting from 5% to 25% of buffer B in 85 minutes, going up to 35% in 10 minutes, then reaching 80% in 5 minutes, and finally maintaining at 80% B for 5 minutes. The eluted peptides were monitored with TripleTOF 5600 System mounted with a Nanospray III source (SCIEX) and a pulled quartz emitter (New Objectives) in sequential window acquisition of all theoretical fragment ion spectra (SWATH), one of data-independent acquisition mode. A 50-ms survey scan (time-of-flight mass spectrometry [MS]) was performed followed by tandem MS (MS/MS) scan windows set with continuous 25 Da windows through 400 to 1200.[19]

Ion Library Generation With Data-Dependent Acquisition

For data analysis of data-independent acquisition MS signals, an ion library was generated. An equal number of peptides from individual samples of both WT and CarnsTg mice were taken and the peptides were pooled. The pooled peptides were loaded onto an XBridge Ethylene Bridged Hybrid column (250×34.6 mm and 130A particle size) and were fractionated using the step gradient elution at a flow rate of 0.5 mL/min (solvent A with 10 mmol/L TEAB, pH 7.5 and solvent B with 100% acetonitrile), 0% to 5% B in 10 minutes, 5% to 35% B in 60 minutes, 35% to 70% B in 15 minutes and 70% B for additional 10 minutes. Before returning to initial

conditions. A total of 30 fractions were collected and individual fractions were delivered to MS for peptide identification. TripleTOF 5600 MS (SCIEX) at data-dependent acquisition mode was employed to identify the peptides with top 20 precursor ions automatically selected for ion fragmentation. The identified peptides from all of the fractions were taken to generate ion library, including retention time, precursor m/z and MS2 spectra, fragment ion m/z, charge state, and relative intensity.

Proteome Quantified With the SWATH Approach

ProteinPilot software (version 4.5, SCIEX) was used to search against a UniProtKB/Swiss-PRot mouse database (Release 2018_04) based on the acquired MS/MS signals at data-dependent acquisition mode. Parameters in the search algorithm of ProteinPilot were configured as cysteine alkylation by iodoacetamide and digestion by trypsin, with biological modifications selected as identification focus. The threshold of the number of proteins for import was set as a false discovery rate of 1% in ProteinPlot. PeakView SWATH Processing Micro App (v2.0, SCIEX) was used to process the SWATH acquisition data and to identify the correct peak group in a set of fragment chromatograms with peaks at the similar retention time with parameters set as: (1) 5000 proteins, (2) 1000 peptides/proteins, (3) 75 ppm m/z tolerance and 30 minutes extraction window, (4) confidence setting 50%, (5) false discovery rate of 1%, (6) shared peptides excluding for SWATH analysis, and (7) modified peptides included. The resulting peak area of each protein after SWATH data processing was exported as quantitative signals.[20]

The data-independent acquisition data of WT (n=3) and cardiospecific CarnsTg (n=3) mice were annotated with SWATH based on the data-dependent acquisition library. Each peptide peak areas were extracted and quantified using QPROT (v1.3.5), with parameter setting: 1) nbumin:2000, niters: 10 000, normalized:1 numThreads: 4. The threshold value of differentially expressed proteins (DEPs) between the 2 types of the samples were defined as >1.5-fold changes in the chromatographic area with significance ($P<0.05$). For missing value processing, the proteins with >50% missing values were removed and the remaining missing values were imputed with kNN. The proteomic data set is available on the iProx database (ID:PXD030647).

Gene Ontology Annotation, Kyoto Encyclopedia of Genes and Genomes Signaling Pathway Analysis, and miRNA Prediction

A gene ontology (GO) annotation database (http://www.geneontology.org) was used to predict gene functions.[21] Functional categories of genes were classified based on early report.[22] The Kyoto Encyclopedia of Genes and Genomes (KEGG; http://www.kegg.jp/) was used to annotate molecular networks. An online miRNA prediction tool, TargetScan, was used to predict the possible miRNA-protein interactions.[23]

Sample Preparation Under Basal Conditions and Global Ischemia

To determine the effects of *Carns* overexpression on the global cardiometabolomic profile under basal conditions, hearts were collected from the WT and CarnsTg mice on euthanization and snap-frozen in liquid nitrogen. To determine the changes in the cardiometabolomic profile associated with the ischemic injury and whether *Carns* overexpression influences the cardiac metabolism, isolated hearts from the WT and CarnsTg mice were perfused in the Langendorff mode for 35 minutes, perfused for 20 minutes followed by 5 minutes of ischemia, and perfused for 20 minutes followed by 15 minutes of ischemia, as previously described.[5] After the experimental protocol, the hearts were collected, snap-frozen in liquid nitrogen, and stored in −80 °C for liquid chromatography with MS/MS analysis.

Global Metabolomics by Gas Chromatography × Gas Chromatography–Mass Spectrometry

WT and CarnsTg mice hearts were processed in a random order to avoid systemic bias. Mice hearts were placed in a 1.5-mL Eppendorf tube, water was added at a ratio of 1:10, and homogenized with glass beads using a Retsch MM 200 model mixer mill (Fisher Scientific). To extract polar metabolites, 800 µL of methanol were added to 200 µL of homogenized heart sample. The mixture was vortexed for 2 minutes and then placed on ice for 10 minutes, followed by another 2 minutes of vortex mixing, and centrifuged at 25 200*g* for 20 minutes at 4 °C. Supernatant was transferred into a glass vial and dried in a SpeedVac evaporator to remove methanol, followed by lyophilization to remove water. The dried metabolite extract was dissolved with 30 µL of 20 mg/mL methoxyamine hydrochloride pyridine solution followed by vigorous vortex mixing for 1 minute. Methoxylation was performed by sonicating the sample for 20 minutes and incubation at 60 °C for 1 hour. Derivatization was performed by adding 20 µL of N-trimethylsilyl-N-methyl trifluoroacetamide (MSTFA) or N-trimethylsilyl-N-methyl trifluroacetamide (MTBSTFA) with 1% trimethylchlorosilane to the glass vial. Samples were incubated for 1 hour at 60 °C and the mixture was transferred to a gas chromatography (GC) vial for analysis. Pooled samples were prepared

by mixing 30 μL of derivatized metabolite extract from each sample to monitor the instrumental variations during the course of gas chromatography × gas chromatography–mass spectrometry (GC×GC–MS) analysis.

The extracted and derivatized samples were analyzed on a LECO Pegasus GC×GC-TOF MS instrument (LECO Corp.) coupled to an Agilent 6890 gas chromatography and a Gerstel MPS2 autosampler (GERSTEL Inc.), featuring a LECO 2-stage cryogenic modulator and secondary oven. The primary column was a 60 m×0.25 mm $^{1}d_{c}$×0.25 μm $^{1}d_{f}$ DB-5 ms GC capillary column (phenyl arylene polymer virtually equivalent to [5%-phenyl]-methylpolysiloxane). The secondary GC column 1 m×0.25 mm $^{2}d_{c}$×0.25 μm $^{2}d_{f}$, DB-17 ms ([50% phenyl]-methylpolysiloxane) was placed inside the secondary GC oven following the thermal modulator. Both columns were obtained from Agilent Technologies and were connected through a press fit connector. The helium carrier gas (99.999% purity) flow rate was set to 2.0 mL/min at a corrected constant flow via pressure ramps. The inlet temperature was set at 280 °C. The primary column temperature was programmed with an initial temperature of 60 °C for 0.5 minutes, then ramped at 5 °C/min to 270 °C and maintained for 15 minutes. The secondary column temperature program was set to an initial temperature of 70 °C for 0.5 minutes and then ramped at the same temperature gradient employed in the first column to 280 °C, accordingly. The thermal modulator was set to 15 °C relative to the primary oven, and a modulation time was 2 seconds. The mass range was set as 29 m/z to 800 m/z with an acquisition rate of 200 mass spectra per second. The ion source chamber was 230 °C with the transfer line temperature of 280 °C, and the detector voltage was 1440 V with electron energy of 70 eV. The acceleration voltage was turned on after a solvent delay of 544 seconds, and the split ratio was set at 10:1.

LECO's instrument control software ChromaTOF (version 4.21) was used for peak picking and tentative metabolite identification, with assignment using the NIST/EPA/NIH mass spectral library (version 2.2) as a reference. Any metabolite assignment with a similarity score <500 (of 1000) was discarded. The analysis results of each sample were exported as a peak list containing the information of the top 10 metabolite assignments for each chromatographic peak. All peak lists were then subjected to MetPP[24–26] software for the first-dimension retention index (^{1}RI) matching with a threshold of $P \leq 0.0001$ (equivalent to an absolute ^{1}RI) difference larger than the threshold discarded. Our in-house database contains the information of 134 authentic metabolites acquired on the same instrument under the same conditions. The information of these authentic metabolites, including the first-dimension retention time ($^{1}t_{R}$), the second-dimension retention time ($^{2}t_{R}$), and EI mass spectrum, was further applied to filter the tentative metabolite assignments, when an authentic metabolite was assigned to a chromatographic peak. A tentative metabolites assignment was considered to be correct only if the experimental information on the authentic metabolite agreed with the corresponding information on the chromatographic peak in the biological samples, ie, the difference of $^{1}t_{R}$ ≤0.05 seconds, and the mass spectral similarity ≥700. After such a putative metabolite identification, peak merging, peak list alignment, normalization, and significant significance test were also performed using MetPP software. R code for generating the volcano plot is described in detail. (https://louisville.edu/medicine/research/cancer/cores-and-facilities-1/biodata/manuscript-code-volcano-plot/view). Biorender.com was used to draw the schemes for the citric acid cycle (TCA). The metabolomic data set is available on metabolic work bench ID Data track:2986.

Western Blot Analysis

Hearts from the WT and CarnsTg mice (n=6 in each group) were homogenized in radioimmunoprecipitation assay buffer (RIPA: 20 mmol/L Tris–HCl pH 7.5, 15 mmol/L NaCl, 1 mmol/L EDTA, 1 mmol/L EGTA, 1% NP-40). For cytosolic fractions, homogenates were centrifuged for 25 minutes at 13 000*g*, and the supernatants were separated by SDS-PAGE. For mitochondrial fractions, the lysate was centrifuged at 700*g* for 15 minutes at 4 °C. The supernatant was recentrifuged at 10 000*g* for 15 minutes at 4 °C, and the mitochondria pellets were resuspended using RIPA buffer (50–100 μL). Immunoblots were analyzed using anti-CARNS1, anti-CPT2, anti-SDH, and anti-ATP synthase β and anti–voltage-dependent anion channel antibodies. Antibodies were purchased from Abcam, Abclonal, and Protein Express. Western blots were developed using horseradish peroxidase substrate (ECL plus from Pierce) and scanned with Biorad ChemiDoc. Band intensity was quantified using Image Quant TL software (Amersham Biosciences) that were normalized to voltage-dependent anion channel and Amido black staining.

Statistical Analysis

For metabolite identification, the maximum spectral similarity score is 1000 and the threshold of spectral similarity score was set as ≥500. The *P* value threshold was set as $P \leq 0.001$ for retention index matching. Partial least squares discriminant analysis (PLS-DA), a supervised technique that uses the partial least squares algorithm to explain and predict the membership of samples to groups, was performed to give an

overview on the metabolic profile difference among groups. A pairwise 2-tailed *t* test with sample permutation was performed between the WT and CarnsTg hearts to determine whether a metabolite had a significant difference in abundance between the 2 groups. Grubbs test was employed for outlier detection before *t* test. The *t* test *P* values were adjusted by up to 1000 times of sample permutation. The threshold of *t* test was set at $P<0.05$. Two-way ANOVA followed by Bonferroni or Tukey posttests were performed to identify the differentially regulated metabolites in the WT and CarnsTg hearts that were subjected to perfusion only and perfusion followed by 5 and 15 minutes of ischemia. The data are normalized using the quantile method. The principal component and volcano plot analyses were performed using SAS (SAS Institute Inc) and R statistical software (The R Foundation). Data are presented as mean±SEM.

Differential expression analysis of RNA-seq data was performed using the NOISeq algorithm.[27] Transcripts with log2 fold change ≥2 and a significant value >0.8 were considered differentially expressed, as per the recommendation of the NOISeq. For proteomics data, DEPs, were calculated using *t* test, with criteria of fold change of ≥2 and a $q<0.05$ were considered statistically significant. Pathway enrichment analysis of both the differentially expressed genes (DEGs) and DEPs were performed based on GO and the KEGG database, and the statistical significance of the pathway was calculated using hypergeometric test. Significantly enriched terms were selected with a $P<0.05$.[28,29]

RESULTS

Identification of DEGs in CarnsTg Hearts

Carns participates in the synthesis of a wide range of histidyl dipeptides such as carnosine, anserine, and carcinine.[1] To examine the effects of increasing the basal levels of this enzyme in the heart, we measured the levels of several histidyl dipeptides in the hearts of WT and CarnsTg mice. As we previously reported,[18] hearts of transgenic mice exhibit normal cardiac function, and showed significantly elevated levels of carnosine and anserine than WT hearts. In addition, the transgenic hearts also had higher levels of homocarnosine than WT hearts. No carcinine was detected either in the transgenic or WT hearts (Figure S1). These observations suggest that Carns overexpression driven by a cardiospecific promoter leads to a selective increase in carnosine, anserine, and homocarnosine in the heart.

To investigate the effects of histidyl dipeptide elevation, we first examined differences in gene expression in WT and transgenic hearts using RNA-seq analysis. The paired-end sequencing of libraries generated 23 983 million sequencing reads, which, after filtering for low quality, generated 23 825 million clean reads. Of the total clean reads, the average mapping ratio of clean reads with reference gene was ≈51.72%; 43.47% were unmapped reads and 4.81% were multiposition match. In comparison with 24 573 (the total number of mouse genes present in the database), we identified 17 509 genes in the WT and 17 468 genes in the CarnsTg mice hearts. Volcano plot of the RNA-seq data indicated the downregulated (negative values) and upregulated (positive values) genes with $\log_2$ (fold change) ≥2 and false discovery rate value <0.001 (Figure 1A).

We next profiled the differential gene expression comparing the WT and CarnsTg hearts, and identified a total of 100 DEGs in the CarnsTg heart, of which 42 were protein-coding genes. In this set, 21 protein-coding genes were upregulated and 21 were downregulated. In the CarnsTg heart, the highly upregulated genes were uncoupling protein 1, carbonic anhydrase 3, phosphoenolpyruvate carboxykinase 1, a predicted gene 38 670, and histone cluster 1 H2ag, and the significantly downregulated genes included fos-like antigen 2, RIKEN complementary DNA, and ladybird homeobox homolog 2. Among the 58 differentially expressed noncoding genes, 29 were upregulated and 29 were downregulated, which included the miRNAs and small nucleolar RNAs. In the miRNA analyses, miR-7067, miR-142, miR-99a, miR-5625, miR-7036, and miR-5621 were highly upregulated in the CarnsTg hearts, and miR-6989, miR-3101, miR-7091, and miR-5111 were significantly downregulated (Figure 1B and Data S1).

To predict biological processes linked to altered gene expression, we functionally annotated all of the 100 DEGs to the GO enrichment analysis. For GO analysis, the annotated genes were divided into 3 major GO categories: cellular component, molecular function, and biological process. In the cellular component, the term of nuclear chromatin was the enriched component. Cellular responses to peptide and chromatin organization were the 2 top biological processes terms, and the most enriched component of the molecular function was DNA binding (Figure 1C). Taken together these results suggest that increasing the myocardial levels of histidyl dipeptides affects the gene profile of heart.

Proteomic Profiling of the WT and CarnsTg Hearts

Although the flow of information from RNA to the protein translation is considered the central dogma, numerous studies have shown that a weak correlation exists between messenger RNA expression and the abundance of translated proteins.[30–34] To determine whether the DEGs in CarnsTg heart could translate at the protein level, we next examined the effect of elevated myocardial histidyl dipeptides on the protein profile and analyzed the differences in protein expression

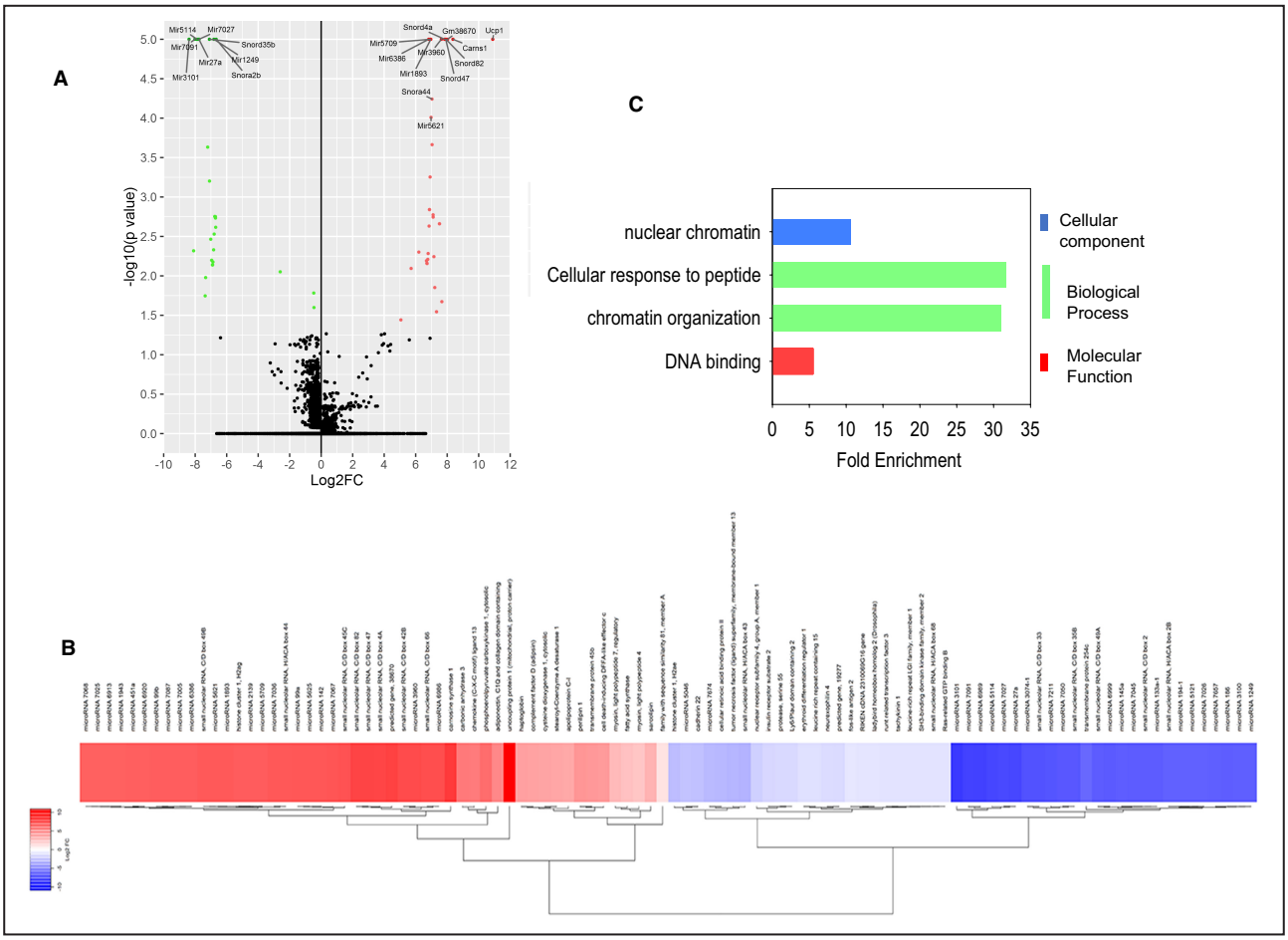

Figure 1. Transcriptomic analysis of the wild-type (WT) and carnosine synthase transgenic (CarnsTg) hearts. **A**, Volcano plot of the transcriptome between the CarnsTg and WT hearts (n=4 mice in each group). Statistical significance $\log_{10}$ of *P* value *y*-axis was plotted against $\log_2$-fold change (*x*-axis). **B**, Heat map of the differentially expressed genes between the CarnsTg and WT hearts. **C**, Gene ontology analysis of the differentially regulated noncoding and coding genes between the CarnsTg and WT mice hearts, which were divided between 3 main categories: cellular component, biological component, and molecular function.

between the WT and CarnsTg mice hearts by proteomic analysis. A total of 4719 and 4743 distinct proteins were identified from the WT and CarnsTg mice hearts, respectively. The DEPs were identified with a q<0.01 and a fold change of ≥2.0 between the WT and CarnsTg hearts. We found that ≈939 proteins were differentially expressed between the WT and CarnsTg mice hearts (Data S2). Of these, 566 were upregulated and 373 proteins were downregulated in the CarnsTg hearts when compared with the WT hearts. Principal component analysis of the DEPs clearly clustered the WT and CarnsTg proteins separately, and unsupervised hierarchical clustering also resulted in grouping of WT and CarnsTg hearts into different clusters. The level of significance and magnitude of changes observed in the proteome by Carns overexpression was visualized by plotting the DEPs on a volcano plot (Figure S2). The highly upregulated proteins in the CarnsTg compared with the WT hearts were the structural proteins such as troponin T, fast skeletal muscle, nebulin, myosin regulatory light chain 2, and titin. Furthermore, many key proteins that were upregulated in the CarnsTg heart were the enzymes involved in the TCA (isocitrate dehydrogenase, and succinate dehydrogenase), fatty acid (FA) transport and metabolism, such as carnitine palmitoyltransferase (CPT) 2, and 2,3 enoyl-CoA hydratase. The significantly downregulated proteins in the CarnsTg compared with the WT hearts were aldehyde dehydrogenase, myosin light chain (MYL) 4, adipsin, and GTPase-activating protein.

To identify changes in specific biochemical pathways, we next annotated the differentially expressed proteins to the NCBI annotation system GO. The GO classification of the upregulated proteins showed that changes in cellular processes and signaling were enriched in posttranslational modification, signal transduction, and cytoskeleton. In the metabolism, energy production and conversion, lipid, amino acid, and carbohydrate transport and metabolism were highly enriched. In the information storage and processing,

translation module-ribosome structure and biogenesis were highly enriched (Figure 2A). In the downregulated proteins, changes in the cellular processes and signaling were linked to signal transduction, posttranslational modification, and cytoskeleton, and in metabolism changes in amino acid transport and metabolism were highly enriched (Figure 2B). We then performed KEGG enrichment analysis to analyze the DEPs, which are shown as scatter plot. KEGG pathway identified that DEPs in the CarnsTg mice hearts were mostly enriched in metabolic pathways, glycolysis, oxidative phosphorylation, FA degradation, cardiac muscle contraction, and TCA (Figure 2C). The KEGG pathway functions associated with the upregulated proteins showed significant differences in the metabolic pathways, thermogenesis, oxidative phosphorylation, cardiac muscle contraction, FA degradation and metabolism, glycolysis, TCA, and pyruvate metabolism. Pathway analysis of the downregulated proteins in the CarnsTg heart were mainly enriched in the metabolic pathways complement and coagulation cascades (Figure 2D). Taken together, these results show that Carns overexpression in the heart enriches the expression of enzymes involved in glycolysis, FA oxidation, and TCA, which could potentially influence cardiac metabolism.

Effect of Carns Overexpression on the Cardiometabolic Profile Under Basal and Ischemic Conditions

To investigate whether the changes observed in the expression of metabolic enzymes in the CarnsTg hearts

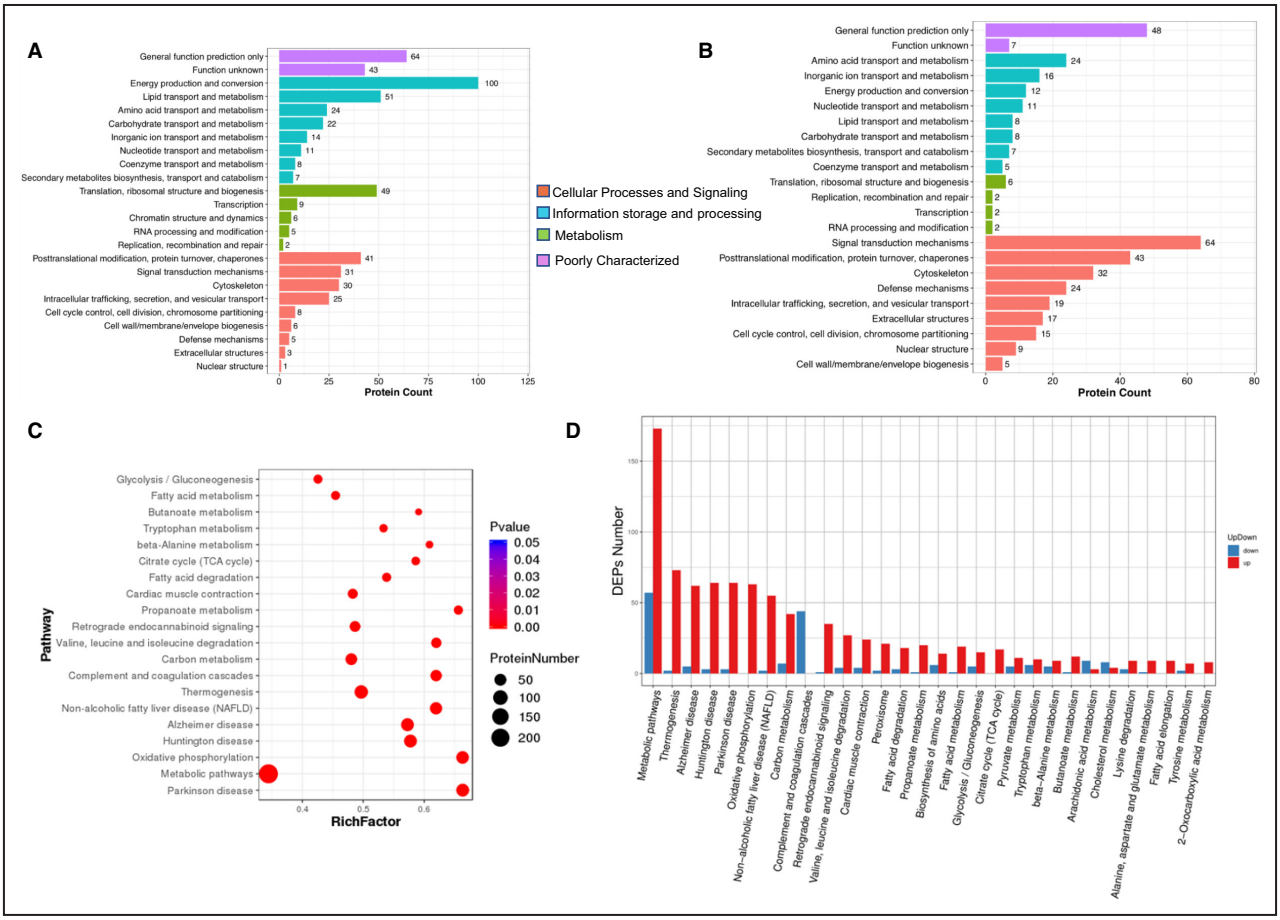

Figure 2. EuKaryotic Ortholog Groups (KOG) of proteins and Kyoto Encyclopedia of Genes and Genomes (KEGG) pathway analysis of the differentially expressed proteins (DEPs) between the wild-type (WT) and carnosine synthase transgenic (CarnsTg) hearts.

The Uniprot IDs of total proteins identified in the WT and CarnsTg hearts (n=3 in each group) via tandem mass spectrometry analysis were used to annotate the proteins with the corresponding KOG annotation. Functional enrichment analysis of (**A**) upregulated proteins showed that the greatest number of these proteins were allocated to metabolism and (**B**) downregulated proteins showed that the greatest number of these proteins were allocated to cellular processes and signaling. **C**, KEGG enrichment analysis: the vertical axis represents the pathway terms with high enrichment and the horizontal axis represents the Rich factor. The size of the q value is represented by the color of the dots. The smaller the q value, the closer the color is towards red. **D**, Enrichment of the specific KEGG pathway annotations for the upregulated (red) and downregulated (blue) proteins in the CarnsTg hearts. TCA indicates citric acid cycle.

could affect cardiac metabolism, we compared the metabolic profiles of WT and CarnsTg hearts under basal and ischemic conditions. For this, polar metabolites from the snap-frozen hearts were extracted and derivatized with MTBSTFA and MSTFA and analyzed, using an unbiased and untargeted global metabolomics approach by GC×GC–MS. Approximately 2700 chromatographic peaks were detected in each of the MTBSTFA-derivatized samples and 3700 chromatographic peaks were detected in the MSTFA-derivatized samples. Approximately 280 and 520 metabolites were identified from the MTBSTFA- and MSTFA-derivatized samples, respectively, including FAs, amino acids, carbohydrates, glycolytic, and citric acid (TCA) intermediates and purines (Datas S3 and S4). PLS-DA of the identified metabolites produced a clear separation between the WT and CarnsTg hearts (Figure S3A and S3B). Volcano plot analysis of the differentially regulated metabolites identified after MTBSTFA and MSTFA derivatizations showed that 16 metabolites were significantly different in the CarnsTg hearts compared with WT hearts. Approximately 12 metabolites were decreased and 4 metabolites were increased in the CarnsTg compared with the WT hearts (Figure 3A and 3B). Significantly, long-chain FA dodecanal and short-chain FAs, such as propanoic acid, as well as the TCA intermediate succinic acid and malic acid were lower in the CarnsTg hearts, when compared with the WT hearts (Table 1), suggesting that increased levels of histidyl dipeptides significantly impacts both FA metabolism and the TCA.

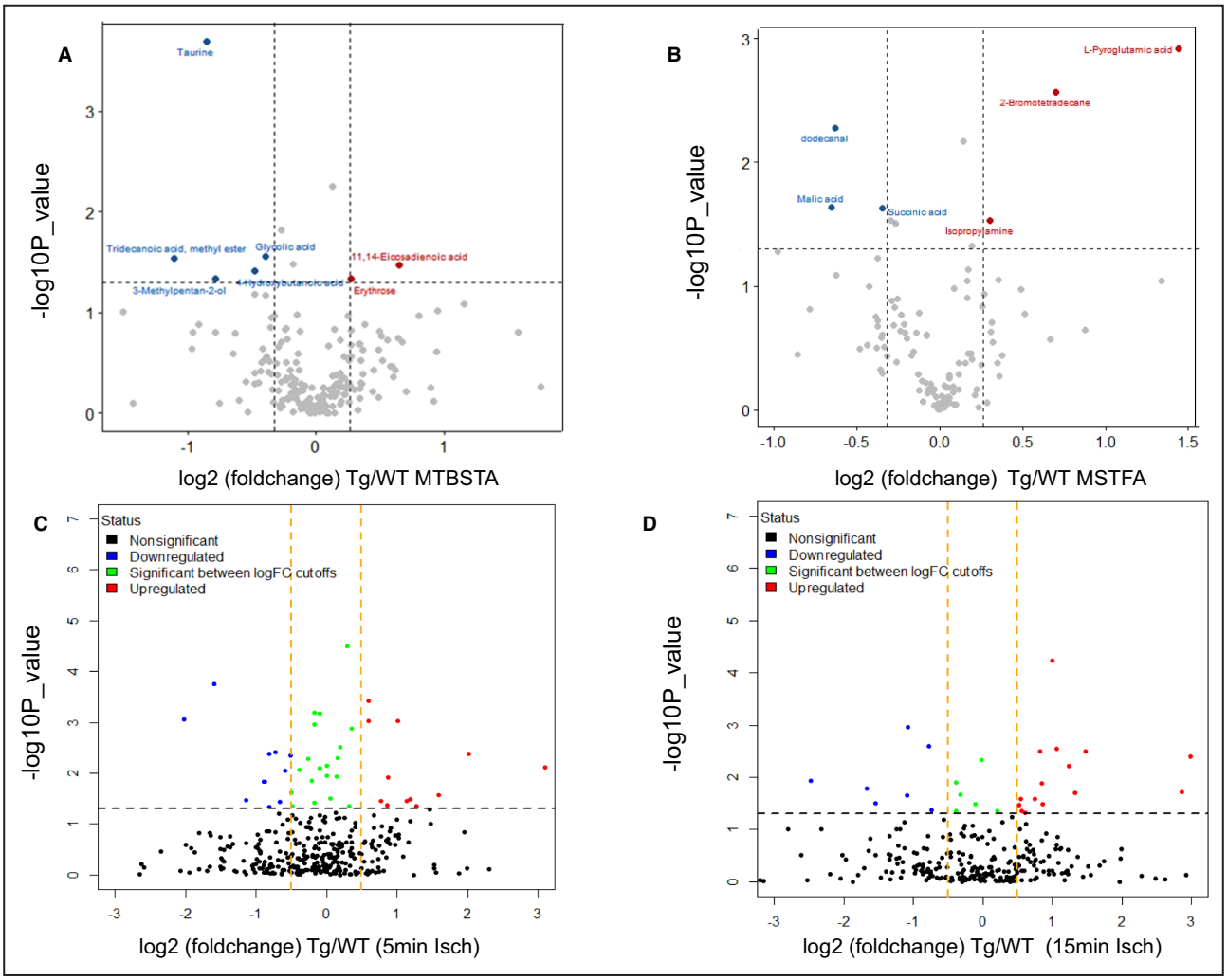

Figure 3. Metabolomic analysis of the wild-type (WT) and carnosine synthase (Carns) transgenic (CarnsTg) hearts under basal conditions and after short durations of ischemia.
Changes in the global cardiometabolomic profile by Carns overexpression were assessed using an unbiased metabolomic approach. **A** and **B**, Volcano plot represents the metabolites identified by N-trimethylsilyl-N-methyl trifluroacetamide (MTBSTFA) and N-trimethylsilyl-N-methyl trifluoroacetamide (MSTFA) derivatization in the WT and CarnsTg hearts under basal conditions. Isolated hearts from the WT and CarnsTg mice were subjected to 5 and 15 minutes of ischemia. The volcano plot represents the metabolites in the WT and CarnsTg hearts identified after (**C**) 5 minutes and (**D**) 15 minutes of ischemia (n=5–7 mice hearts in each group).

Table 1. Metabolites Altered by Carns Overexpression in the Heart Under Basal Conditions That Were Detected by MTBSTFA and MSTFA Derivatization

No	Metabolites	*P* value	Fold change	Change
1	Taurine	0.002	0.55	Decrease
2	Amino butyric acid	0.031	0.83	Decrease
3	Carbonic acid	0.05	0.51	Decrease
4	Glycolic acid	0.025	0.76	Decrease
5	Erythrose	0.032	1.16	Increase
6	4-Hydroxybutanoic acid	0.038	0.72	Decrease
7	11,14-Eicosadienoic acid	0.035	1.56	Increase
8	3-Methylpentan-2-ol	0.045	0.58	Decrease
9	Dodecanal	0.005	0.65	Decrease
10	Catechol	0.021	0.64	Decrease
11	Succinic acid	0.022	0.79	Decrease
12	Isopropylamine	0.027	1.23	Increase
13	Pyroglutamic acid	0.001	2.72	Increase
14	Amino oxy acetic acid	0.05	0.77	Decrease
15	Propanoic acid	0.028	0.81	Decrease
16	Malic acid	0.023	0.64	Decrease

Carns indicates carnosine synthase; MSTFA, N-trimethylsilyl-N-methyl trifluoroacetamide; and MTBSTFA, N-trimethylsilyl-N-methyl trifluroacetamide.

Next, to examine whether increased myocardial levels of histidyl dipeptides affect the cardiometabolic profile during ischemia, which is independent of any neurohormonal effects, we subjected the isolated WT and CarnsTg hearts to different durations of global ischemia in the Langendorff mode. Hearts from WT and CarnsTg mice were perfused for either: (1) 35 minutes, and (2) for 20 minutes followed by either 5 minutes or (3) 15 minutes of global ischemia. The hearts were then immediately frozen for measuring metabolites. Using an unbiased and untargeted global metabolomics approach, ≈260 metabolites were identified. Analysis of the WT and CarnsTg perfused only (35 minutes) hearts showed that ≈26 metabolites were different between the 2 groups (Data S5). PLS-DA of the metabolic profiles produced a clear separation between the WT and CarnsTg hearts (Figure S4A). Volcano plot analysis showed that the abundance levels of several metabolites such as pyroglutamic acid and ribitol were increased, whereas several FAs, such as palmitic acid and arachidonic were decreased and increased respectively in the CarnsTg hearts (Figure S4B and Data S5). To examine the influence of *Carns* overexpression on the global metabolomic profile in response to 5 minutes of global ischemia, we next created a PLS-DA plot with the samples classified into 4 groups: WT and CarnsTg hearts (perfusion only) and WT and CarnsTg hearts (20 minutes perfusion and 5 minutes ischemia), which showed that the ischemia caused a significant deviation from the perfused hearts (Figure S5A). Analysis of the metabolomic profiles between the WT-perfused and ischemic hearts showed that ≈110 metabolites were significantly different after 5 minutes of ischemia, resulting in a significant reduction in amino acids (aspartic acid, proline, and norleucine), accumulation of free FAs (FFAs; palmitic acid, nonanoic acid, and decanoic acid), and decreases in the metabolites of FA (3-hydroxybutyric acid) and intermediates of TCA (oxaloacetic acid; Data S5). Metabolomic profiling between the WT and CarnsTg ischemic hearts (5 minutes) showed that ≈25 metabolites were significantly different between the 2 groups (Table 2). Volcano plot analysis showed that the levels of FFAs (decanoic acid and stearic acid) were lower and pyruvic acid––the metabolite of glycolysis––was increased

Table 2. Metabolites Significantly Altered in the CarnsTg Compared With the WT Hearts After 5 Minutes of Global Ischemia

No.	Metabolite	*P* value	Fold change	Change
1	4-Ketoglucose	0.005	1.19	Increase
2	Nonanoic acid	0.027	0.31	Decrease
3	Gluconic acid	0.044	1.39	Increase
4	2,3 Butanediol	0.014	1.84	Increase
5	Slidenafil	0.032	0.43	Decrease
6	Decanoic acid	0.442	0.41	Decrease
7	Erythrono-1,4 lactone	0.008	1.34	Increase
8	Erythro-pentonic acid	0.009	0.49	Decrease
9	Methyl galactosidase	0.001	0.81	Decrease
10	2-Ketohexanoic acid	0.009	4.05	Increase
11	L-Threonic acid	0.043	0.54	Decrease
12	Ethyl-D-glucopyranoside	0.007	0.11	Decrease
13	D-Glucose	0.009	0.66	Decrease
14	Pyridine	0.007	1.13	Increase
15	Propargyl alcohol	0.011	1.00	Increase
16	L-Proline	0.043	0.85	Decrease
17	Butanal	0.04	1.76	Increase
18	Pantalactone	0.001	1.12	Increase
19	Acetic acid	0.004	1.75	Increase
20	Pyruvic acid	0.007	1.10	Increase
21	Phosphonic acid	0.0031	0.86	Decrease
22	Glycerol 3-phosphate	0.023	1.40	Increase
23	11,14 Eicosanoic acid	0.007	0.93	Decrease
24	Stearic acid	0.007	0.68	Decrease
25	d-Mannose	0.0042	4.06	Increase
26	Dodencanoyl chloride	0.041	1.15	Increase
27	Methylamine	0.031	1.57	Increase
28	Decanoic acid	0.03	0.57	Decrease
29	Fumaric acid	0.09	1.29	Increase

CarnsTg indicates carnosine synthase transgenic; and WT, wild-type.

Table 3. Significantly Altered Metabolites in the CarnsTg Compared With the WT Hearts After 15 Minutes of Ischemia

No.	Metabolite	*P* value	Fold change	Change
1	2-Pyrrolidinone	0.011	2.104	Increase
2	D-Mannose	0.006	0.42	Decrease
3	Decanoic acid	0.042	0.6	Decrease
4	9-Octadecenoic acid	0.0040	0.12	Decrease
5	4-Aminobutanoic acid	0.011	5.54	Increase
6	Fumaric acid	0.031	2.91	Increase
7	Mercaptoacetic acid	0.032	0.55	Decrease
8	D-Glucose	0.020	0.39	Decrease
9	Ribitol	0.020	1.25	Increase
10	Phosphonic acid	0.006	0.50	Decrease
11	Pyroglutamic acid	0.04	1.31	Increase
12	Arachidonic acid	0.04	1.31	Increase
13	Pyruvic acid	0.02	0.59	Decrease
14	2-Keto-hexanoic acid	0.02	2.12	Increase

CarnsTg indicates carnosine synthase transgenic; and WT, wild-type.

in the CarnsTg compared with the WT ischemic hearts (Figure 3C). Significantly, the levels of 2,3-butanediol were decreased in the CarnsTg ischemic hearts following 5 minutes of ischemia. 2,3 Butanediol is formed by the reduction of acetoin (3-hydroxybutan-2-one), a minor metabolite of pyruvate and an early marker of ischemia.[35,36]

To identify the effects of histidyl dipeptides on the cardiometabolic profile, during longer durations of ischemia, we subjected the WT and CarnsTg hearts to either 35 or 20 minutes of perfusion, followed by 15 minutes of ischemia. PLS-DA plot of the 4 groups: WT and CarnsTg hearts (perfusion only) and WT and CarnsTg hearts (20 minutes perfusion and 15 minutes ischemia), produced a clear separation of the groups (Figure S5B). We found that 63 metabolites were significantly altered in the WT ischemic hearts, which belonged to the FA and amino acid metabolism and TCA. Levels of ketone bodies, such as 3-hydroxybutyric acid, markers of ischemic injury 2,3 butanediol were increased in the ischemic WT hearts (Data S5). We also identified 17 metabolites that were significantly different between the WT versus CarnsTg ischemic hearts following 15 minutes of ischemia (Table 3). Intermediates of TCA-fumaric acid and glycolysis-pyruvic acid were higher in the CarnsTg hearts compared with the WT ischemic hearts (Figure 3D). Similarly, the levels of FA (decanoic acid and arachidonic acid) were decreased in the ischemic CarnsTg hearts. Taken together, the global metabolic analysis of the CarnsTg hearts suggests that the enrichment of enzymes involved in β-FA oxidation and TCA by Carns overexpression could improve cardiac fuel utilization.

Metabolic Pathway Analysis

Given that Carns overexpression affects several different metabolic pathways, under both basal and ischemic conditions, we next performed pathway analysis of the metabolites identified by MTBSTFA and MSTFA derivatization. This analysis showed that under the basal conditions, biochemical pathways involved in the metabolism of pentose phosphate pathway, valine, leucine, and isoleucine, as well as arginine biosynthesis were different between the CarnsTg and WT hearts (Figure 4A and 4B). Pathway analysis of the significantly different molecules, identified 2- to 3-fold enrichment in the TCA, glycolysis, biosynthesis of unsaturated FAs, and 10- to 15-fold enrichment in the phenylalanine, tyrosine, and tryptophan metabolism (Figure 4C and 4D).

Next, we examined the metabolic pathways affected by ischemia in the WT and CarnsTg hearts. In the perfused hearts of the WT and CarnsTg mice, metabolic analysis revealed that *Carns* overexpression affected pyruvate metabolism and glycolysis and enriched pyruvaldehyde degradation (Figure S4C and S4D). Metabolic analysis revealed that 5 minutes of ischemia in the WT hearts induced perturbations in the TCA, FAs, and amino acid metabolism (Figure S6A). Pathway enrichment analysis of the metabolites, which were significantly different, identified 4- to 10-fold enrichment in the malate–aspartate shuttle, urea cycle, and aspartate metabolism (Figure S6B). Similarly, prolonged ischemia of the WT mice hearts (15 minutes) induced significant perturbations in the TCA and amino acid metabolism, and significant enrichment of the malate–aspartate shuttle (Figure S6C and S6D). To examine the metabolic pathways, which are affected by *Carns* overexpression in the ischemic heart, pathway analysis of the metabolites that are different between the CarnsTg and WT mice hearts following 5 minutes of ischemia indicated significant differences in glycolysis, TCA, FA biosynthesis, pyruvate, butanoate, arginine, and proline metabolism (Figure 4E). Enrichment analysis identified ≈2- to 8-fold enrichment in pyruvaldehyde degradation, β-oxidation of very long-chain FAs, alanine and cysteine metabolism, glucose-alanine cycle, glycolysis, and TCA (Figure 4G). Furthermore, pathway impact analysis of metabolites, which were differentially affected following 15 minutes of ischemia between the WT and CarnsTg hearts, showed that the highest pathway impact for the CarnsTg ischemic hearts was caused by the TCA, alanine, aspartate, and glutamate metabolism (Figure 4F). Enrichment analysis of these metabolites identified 5- to 8-fold differences in the glucose-alanine cycle, pyruvaldehyde degradation, transfer of acetyl groups into

mitochondria, TCA, and glycolysis between the WT and CarnsTg hearts (Figure 4H). Collectively, these data suggest that Carns overexpression in the heart influences and improves multiple metabolic pathways under both aerobic and anaerobic conditions, in particular the utilization of glucose and FAs.

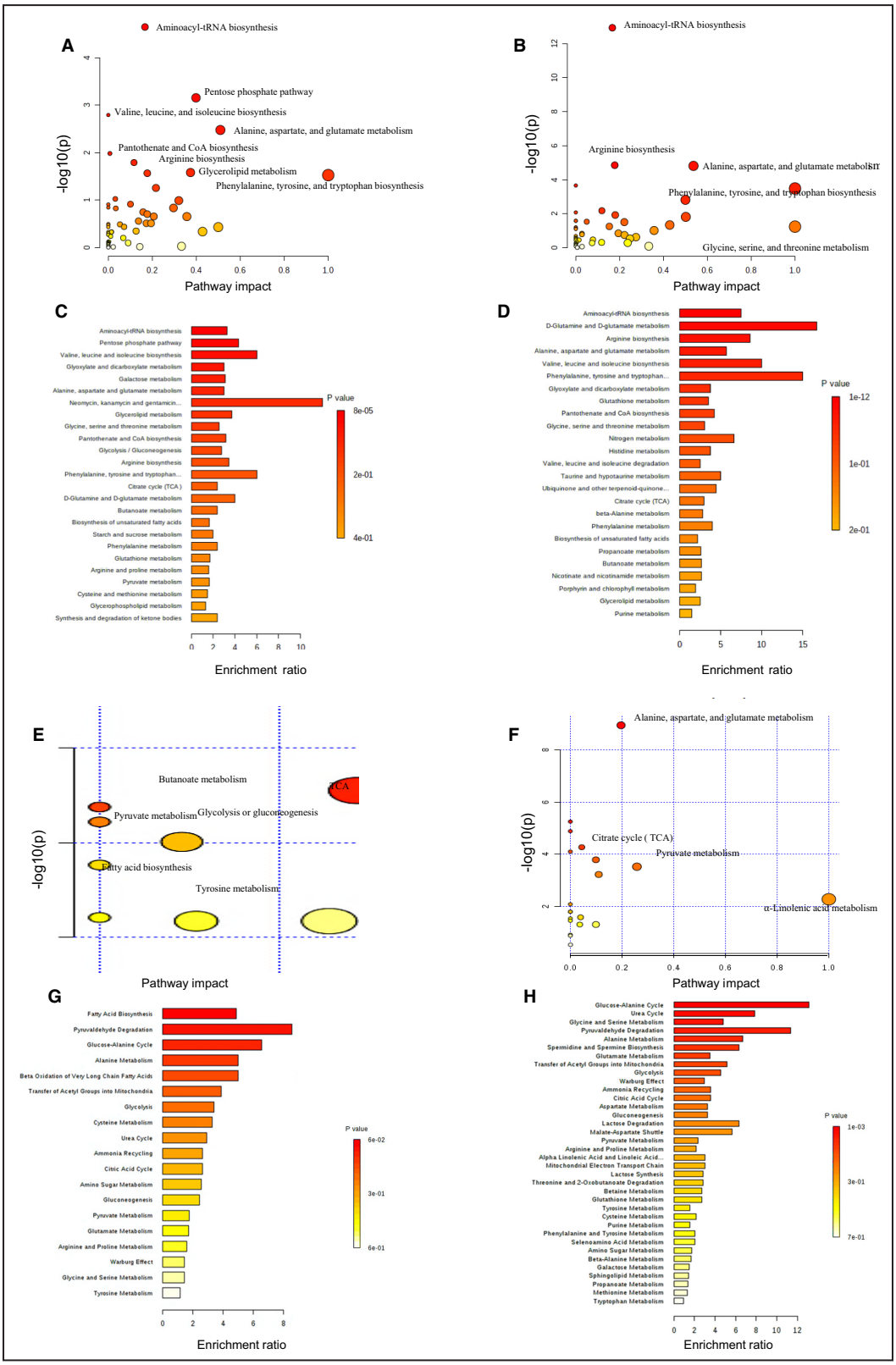

Figure 4. Pathway impact and enrichment of the differentially regulated metabolites in the wild-type (WT) and carnosine synthase transgenic (CarnsTg) hearts under basal and ischemic conditions.
A and **B**, Pathway impact analysis, and (**C** and **D**) pathway enrichment of the differentially regulated metabolites identified by N-trimethylsilyl-N-methyl trifluroacetamide and N-trimethylsilyl-N-methyl trifluoroacetamide derivatizations, respectively, between the WT and CarnsTg mice hearts under basal conditions. Pathway impact analysis after (**E**) 5 minutes and (**F**) 15 minutes of ischemia, and pathway enrichments of the differentially regulated metabolites (**G**) after 5 minutes and (**H**) 15 minutes of ischemia, between the WT and CarnsTg mice hearts (n=5–7 hearts per group). TCA indicates citric acid cycle.

Integration of the Transcriptomic, Proteomic, and Metabolic Networks

Given that the effects of histidyl dipeptides were observed at the gene, protein, and metabolite levels, we next integrated the transcriptomic, proteomic, and metabolomic data sets and identified the levels of interaction between the 3 data sets. We first correlated the 42 DEGs and 810 DEPs and found that none of the DEGs and DEPs overlapped or correlated with each other. Since most of the DEGs did not correlate with the DEPs, we next performed the in-silico analysis between the highly regulated DEPs with the differentially expressed miRNAs using the TargetScan (Whitehead Institute for Biomedical Research). We found that miR-5046, which was downregulated in the CarnsTg heart, targets the expression of highly DEP troponin T3 fast skeletal muscle. Similarly, miR-6989 and miR-3100, which were decreased in the CarnsTg hearts, targets the expression of succinate dehydrogenase and 2,3 enoyl-CoA hydratase, respectively. Further, miR-6913 increased in the CarnsTg hearts was predicted to target aldehyde dehydrogenase (Table 4).

To uncover the potential interactions between the DEPs and metabolites in the CarnsTg hearts, we compared the proteomics and metabolomics clusters for enriched GO term and KEGG pathways. Based on the KEGG pathway analysis, β-FA oxidation and TCA pathways enriched at the protein levels were paralleled with the high enrichment of β-FA oxidation and TCA at the metabolite levels. The main enzymes regulating the abundance of FFAs are FA synthase, long-chain acyl CoA synthetase, CPT1 and 2, and 4 enzymes involved in β-FA oxidation including acyl-CoA dehydrogenase, 2,3 enoyl CoA hydratase, 3 hydroxyacyl CoA dehydrogenase and 3-ketoacyl-CoA thiolase. Our proteomic screening identified all of the major transporters and enzymes involved in regulating FAs (Data S2). We found that the expression of CPT2, and all of the 4 enzymes involved in β-oxidation of FAs, were higher in the CarnsTg hearts than the WT hearts (Figure 5A through 5E). Increase in the expression of CPT2 was further validated by Western blot showing that CPT2 was increased in the CarnsTg hearts compared with the WT hearts (Figure S7A). In parallel with the increase in the expression of enzymes involved in FA oxidation, global metabolomic profiling at baseline showed that the levels of FFAs and dodecanal and propanoic acid were decreased in the CarnsTg hearts (Table 1). Similarly, following 5 minutes of ischemia, decanoic acid and stearic were decreased in the CarnsTg hearts (Figure 5F and 5G). Furthermore, the intermediates of TCA, succinic acid and fumaric acid, were decreased and increased in the CarnsTg hearts under the basal conditions and following 15 minutes of ischemia, respectively. Mirroring the changes in TCA intermediates, proteomic analysis showed that the expression of succinate dehydrogenase, which oxidizes succinate to fumarate, was increased in the CarnsTg hearts (Figure 6A through 6D), which was further confirmed by Western blot analysis (Figure S7B). In addition, our integration analysis of the 3 data sets showed that the decrease in glycolic acid was mirrored by decreased expression of aldehyde dehydrogenase in the CarnsTg hearts (Figure 6E and 6F). Western blot analysis further confirmed that aldehyde dehydrogenase expression was decreased in the CarnsTg hearts compared with WT mice hearts (Figure S7A). Integration of the KEGG pathway database and TargetScan analysis showed that 3 miRNAs (6989, 3100, and 6913) could target the expression of 3 proteins (succinate dehydrogenase, 2,3 enoyl-CoA hydratase, and aldehyde dehydrogenase), belonging to β-FA oxidation, TCA, and ethylene glycol pathways. Collectively, our triomic analysis shows, for the first time, synergistic networks at the transcriptome, proteome, and metabolome levels,

Table 4. Target Proteins of Differentially Regulated miRNA

miRNA	Change	Putative target gene	Protein	Change
mmu-miR-5046	Decrease	Tnnt3	Troponin T3 fast skeletal muscle	Increase
mmu-miR-5046	Decrease	Casq2	Calsequestrin	Increase
mmu-miR-6913	Increase	Aldh2	Aldehyde dehydrogenase	Decrease
mmu-miR-6989	Decrease	Sdha	Succinate dehydrogenase	Increase
mmu-miR-3100	Decrease	Echs1	2,3 enoyl-CoA hydratase	Increase

miRNA indicates microRNA.

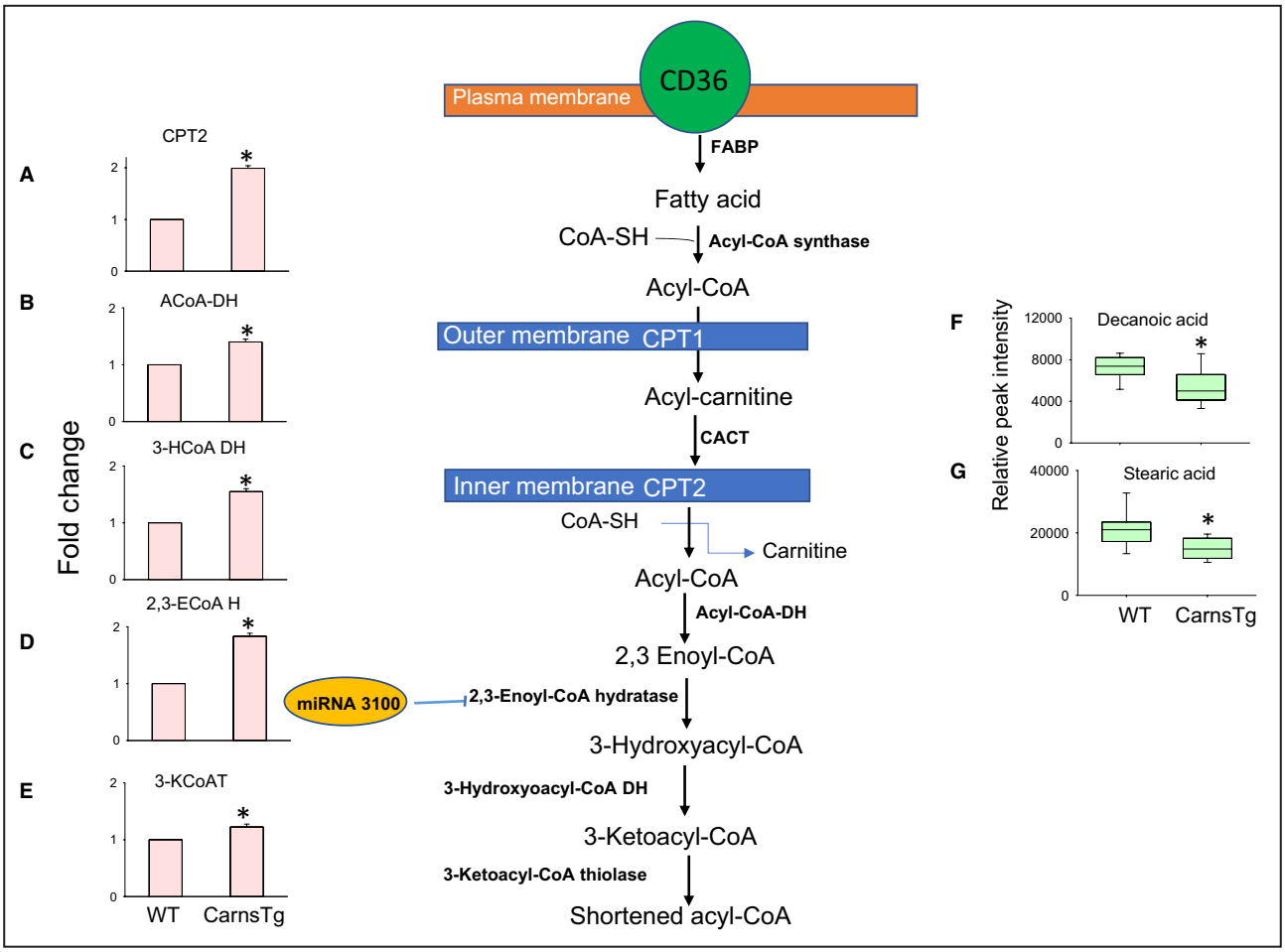

Figure 5. Transcriptomic, proteomic, and metabolic interactions of the fatty acid metabolism in the carnosine synthase transgenic (CarnsTg) hearts.
Schematic overview of the fatty acid metabolism, potential target of miRNA-3100, and levels of detected metabolites and proteins in the wild-type (WT) and CarnsTg hearts. Relative fold changes in the expression of (**A**) Carnitine palmitoyltransferase 2 (CPT2), (**B**) acyl-CoA hydratase (ACoA-DH), (**C**) 3-hydroxyacyl-cCoA dehydrogenase (3HCoA DH), (**D**) 2,3 enoyl-CoA hydratase (2,3-ECoAH), and (**E**) 3-ketoacyl-CoA thiolase (KCoAT) between the WT and CarnsTg hearts. Free fatty acid levels (**F**) decanoic acid and (**G**) stearic acid in the WT and CarnsTg hearts following 5 minutes of global ischemia. *$P<0.05$ vs WT (n=4–8 mice in each group). FABP indicates fatty acid–binding protein; and miRNA, microRNA.

by which histidyl dipeptides could optimize the cardiac fuel utilization under aerobic and anaerobic conditions (Figures 5 and 6).

DISCUSSION

In the present study we adopted a multilayer omics approach to characterize in detail the genomic and proteomic changes that occur as a result of an increase in myocardial histidyl dipeptide levels and then investigated their effects on the global metabolic profile, under both aerobic and anaerobic conditions. Moreover, we combined the RNA-seq, global proteomics, and untargeted metabolomics data sets to identify the metabolic pathways that exhibited correlative changes on all 3 levels. Transcriptomic analysis showed that genes associated with chromatin organization and DNA binding, as well as miRNAs that could target the expression of enzymes associated with β-FA oxidation and TCA were differentially regulated by histidyl dipeptides. Proteomic analysis showed that the abundance of ≈939 proteins regulating different cellular, signaling, and metabolic processes was affected by Carns expression. In particular, the abundance of several enzymes involved in β-FA oxidation and TCA were enriched in CarnsTg hearts. Our metabolic profiling showed that the levels of FFAs were decreased and the intermediates of TCA, such as fumaric acid, were increased in the transgenic hearts under anaerobic conditions. Integration of the 3 data sets provided a comprehensive understanding of how interactions at miRNA and protein levels could optimize the utilization of cardiac fuels, particularly FAs and glucose, under physiological

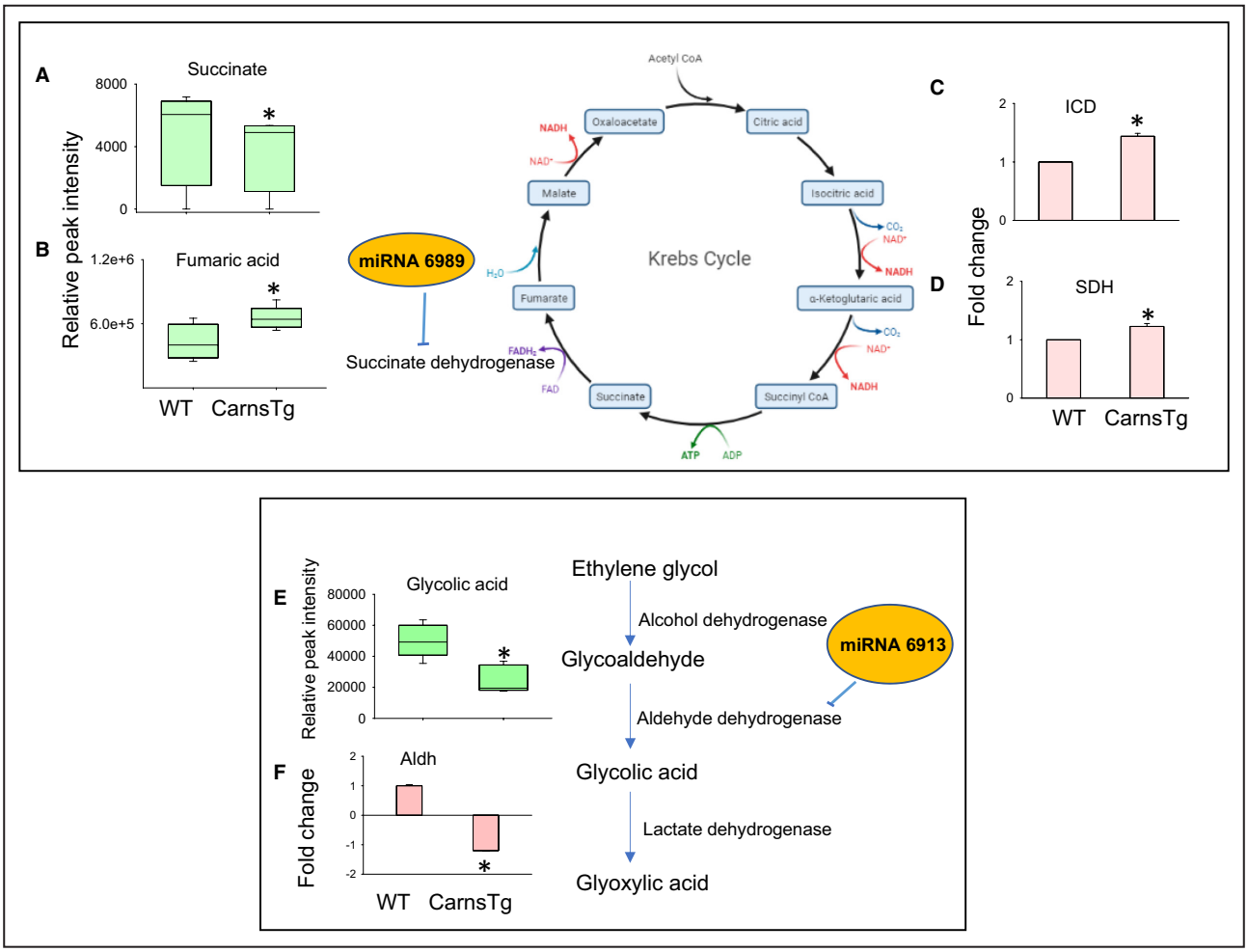

Figure 6. Transcriptomic, proteomic, and genomic interactions in the carnosine synthase transgenic (CarnsTg) hearts. Schematic overview of the citric acid cycle (TCA), potential target of microRNA (miRNA)-6989, and levels of TCA intermediates. **A**, Levels of succinic acid under basal conditions and (**B**) fumaric acid following 15 minutes of ischemia. Relative fold changes in the expression of (**C**) isocitrate dehydrogenase (ICD) and (**D**) succinate dehydrogenase (SDH) between the WT and CarnsTg hearts. Schematic for glyoxylic acid formation and potential target of miRNA-6913. Levels of (**E**) glycolic acid and (**F**) expression of aldehyde dehydrogenase (Aldh) in the WT and CarnsTg hearts. *P<0.05 vs WT (n=4–8 mice in each group). WT indicates wild type.

and pathological conditions in the transgenic heart. Collectively, these results provide, for the first time, an integrated view of the genomic, proteomic, and metabolomic changes affected by histidyl dipeptides in the heart. More broadly, results of concurrent genomic, proteomic, and metabolic analyses highlight the limitation of these approaches individually, and illustrate how a combination of different approaches could provide a more comprehensive analysis of metabolic changes than each of these approaches individually.

Role of Histidyl Dipeptides in Gene and Protein Regulation

Our omics analyses indicated that ≈100 coding and noncoding genes and 938 proteins were differentially expressed in the CarnsTg heart and none of the DEGs and DEPs were correlated at both the gene and protein levels in transgenic hearts. Among the most marked DEPs observed in the transgenic hearts were troponin complex (I and T), which increased 3- to 4-fold relative to the WT hearts. It is interesting to note that *Carns* overexpression causes a switch and increases the expression of fast skeletal muscle troponin in the heart. A number of regulatory networks such as thyroid hormone,[37] transcription factors,[38] and miRNAs[39] could regulate the expression of cardiac, slow twitch, and fast twitch contractile protein gene isoforms to the respective muscle type. Analysis of the data using an miRNA target prediction tool indicated that troponin T3 fast skeletal muscle is the possible target of miRNA-5046, suggesting that the downregulation of miRNA-5046 could switch and increase the expression of fast skeletal muscle in the CarnsTg hearts, without discernable changes in the gene expression per se. Nevertheless, further investigations are required to

confirm the presence of specific miRNA-protein interactions, and to garner more in-depth understanding of the mechanisms by which posttranscriptional regulation of proteins is influenced by histidyl dipeptides.

One of the key findings of this work that was not previously described is the enrichment of cardiac muscle contraction pathway in the transgenic heart. The cardiac contractility is a complex machinery of cellular proteins, which includes tropomyosin α1 chain (TPM1); MYL1, MYL2, MYL3, and MYL4; MHC6 and MHC7; and ATPase sarcoplasmic/endoplasmic reticulum. Our proteomic analysis showed that the expression of MYL1, MYL2, MYL3, MHC7, troponin, and calsequestrin were increased in the transgenic hearts. A critical key to the pathogenesis of heart failure is decreased expression of proteins involved in the contractile machinery, such as titin and MYL.[40] Previous reports show that MYL2 is decreased in failing hearts[41] and mutation in the MYL2 lead to cardiomyopathy.[42] Because contractile function of the heart is the most important cardiac function and disruption of different sarcomeric proteins expression contributes towards cardiac dysfunction, upregulation of contractile machinery in the CarnsTg heart could possibly contribute to preserving contractile dysfunction in failing hearts.

Role of Histidyl Dipeptides in Basal Myocardial Metabolism

In our previous work we found that increasing the endogenous levels of histidyl peptides increases intracellular pH buffering. This increase in buffering capacity allows the heart to maintain glycolysis during ischemia, generate higher levels of ATP, and undergo less severe ischemic injury than the hearts with lower buffering capacity.[18] However, in addition to intracellular buffering, histidyl dipeptides can also affect other metabolic pathways. Previous studies show that carnosine induces the expression of pyruvate dehydrogenase,[8] suggesting that these ancillary changes may also be essential for preserving glycolysis or may have independent effects that may provide additional protection to the heart. Hence, to obtain a more holistic view of the metabolic effects of histidyl dipeptides, we performed an unbiased global metabolic profiling and found that 16 metabolites were significantly different in CarnsTg mice hearts. We found that the levels of succinate, a TCA intermediate, were lower in the transgenic hearts than in the WT hearts. Concordant with this decrease, our proteomics analysis showed that in comparison with WT hearts, the transgenic hearts had increased expression of TCA enzymes, particularly succinate dehydrogenase, which oxidizes succinate to fumarate. Succinate is recognized as a universal metabolic signature of ischemic injury, which accumulates in the ischemic tissues on reperfusion and drives a burst of reactive oxygen species production by mitochondrial complex I.[43] Hence, the decrease of succinate in the transgenic heart under basal conditions could potentially mitigate reactive oxygen species production and ameliorate oxidative stress injury, when subjected to ischemia, and thereby account for the better contractile recovery of transgenic hearts after ischemia.[18]

A key finding of this study is that levels of long-chain FA dodecanal, as well levels of short-chain FAs, such as propionic acid and 4-hydroxybutanoic acid, were lower in the CarnsTg hearts than the WT hearts. FAs enter the cell via FA protein transporters, such as FA translocase (CD36).[44] Then, a family of FA-binding proteins facilitate FA transport into cardiomyocytes.[45] FFAs are activated to form fatty acyl-CoAs, which are subsequently imported via the mitochondrial matrix by the carnitine shuttle system. CPT1, located in the outer membrane of mitochondria, forms fatty acyl carnitine, which is translocated into the mitochondrial membrane by carnitine-acylcarnitine translocase.[44] Fatty acyl carnitine is converted back to fatty acyl CoA by CPT2 located on the mitochondrial membrane.[44,46] In the mitochondria, β-oxidation of FA is catalyzed by 4 enzymes: acyl-CoA dehydrogenase, 2,3 enoyl CoA hydratase, 3-hydroxyacyl CoA dehydrogenase, and 3 ketoacyl-CoA thiolase. Although our proteomic analysis showed no change in the expression of CD36, the abundance of CPT2 and the 4 enzymes involved in the FA oxidation was significantly higher in the transgenic hearts than the WT hearts, suggesting that the enrichment of β-FA oxidation in CarnsTg hearts observed at the proteome level could potentially contribute towards decreasing FFA levels.

The expression of FA transporters and enzymes involved in β-FA oxidation are largely under the transcriptional control of PPARα and PPARδ, the retinoid X receptor-α, and PPAR coactivator γ.[47] Previously, it was reported that β-alanine, a precursor for carnosine, increased PPARδ expression, suggesting that histidyl dipeptides could be the natural PPAR ligands.[15] In addition, our in vivo silico analysis showed that miRNA-3100 decreased in the CarnsTg hearts could target the expression of 2,3 enoyl-CoA hydratase. However, further studies are needed to confirm how these naturally occurring histidyl dipeptides affect the expression and activity of transcription factors and also to validate whether the miRNAs affected by Carns overexpression could target the expression of enzymes involved in β-FA oxidation. Nonetheless, our results thus far indicate that multiple metabolic pathways are affected by enhancing myocardial histidyl dipeptides. Significantly in the CarnsTg hearts, the decrease in FFAs is accompanied by an increase in the expression of enzymes involved in β-FA oxidation, suggesting that higher levels of histidyl dipeptides are conducive to or permissive of FA oxidation even in a nonstressed, nonischemic heart.

Role of Histidyl Dipeptides in the Ischemic Heart

Metabolic derangement is a key feature of cardiac ischemic injury. Multiple studies have shown that a progressive decrease of glucose and FA utilization is a characteristic signature of ischemic hearts.[46,48–50] Elevated levels of circulating FFAs in the ischemic heart are associated with an increased incidence of ventricular arrhythmias, postinfarction angina, and mortality in patients with acute myocardial infarction.[46,51,52] High levels of FFAs are also common in patients who have myocardial ischemia. Studies in animal models of regional and global ischemia show that excess FA accumulation in the heart impairs ventricular function. Such accumulation of FFAs during ischemia, particularly long-chain fatty acyl-CoA and long-chain acylcarnitine esters, weakens the membrane and compromises the function of membrane-bound proteins. It has also been associated with increased mitochondrial membrane permeability, changes in calcium homeostasis, suppression of glucose utilization, and increased myocardial oxygen consumption in ischemic hearts.[53–55] In view of these findings, it has been suggested that decreasing the uptake and utilization of FAs could be a potential strategy to salvage the ischemic myocardium. Although inhibiting the mitochondrial uptake of FA by inhibiting CPT1 improves postischemic contractile function,[56–58] which is independent of decreasing FA utilization,[59] decreasing FA oxidation under conditions of elevated FA availability leads to the accumulation of toxic lipid intermediates including diacylglycerol, which causes aberrant cardiac signaling and toxicity.[44,60–64] In the present study, we found that FFAs (nonanoic acid and decanoic acid) were increased in the isolated WT ischemic hearts, suggesting that the accumulation of FFAs is independent of their uptake and transport. We also found that Carns overexpression increased the utilization of FFAs and glucose, which was marked by decreases in the levels of stearic and decanoic acid and an increase in the pyruvic acid levels. This favorable profile could, in turn, attenuate ischemic injury by preventing FFA-induced changes in cardiac signaling, metabolism, and mitochondrial function.

We previously reported that Carns overexpression delays myocardial acidification during ischemia, which facilitates glucose metabolism via glycolysis.[18] In the current study, our proteomic analysis showed that Carns overexpression increases the expression of the FA transporters and enzymes involved in FA metabolism. Therefore, the improvements in the FA utilization observed under the ischemic conditions in the CarnsTg ischemic hearts could be either secondary to the improvements in pH and glucose utilization or attributable to the increase in the expression of β-FA oxidation enzymes. In addition to FFA accumulation, ischemia also induces substantial changes in the TCA intermediates. It has been reported that the loading of TCA intermediates, such as fumarate, protects the heart from ischemia–reperfusion injury. In studies with mice deficient in fumarate dehydratase, increases in cardiac fumarate levels are associated with marked reduction in infarct size.[65] Our results show that fumaric acid was increased in the ischemic CarnsTg heart, which was mirrored by the increased expression of the succinate dehydrogenase that catalyzes the oxidation of succinate into fumarate. Taken together, the results of our metabolomic and proteomic profiling suggest that Carns overexpression increases the expression of β-FA oxidation enzymes and is accompanied by an increase in FA and glucose utilization. Collectively these findings suggest that during ischemia, the elevated levels of histidyl dipeptides support the channeling of both the cardiac fuels, glucose and FAs, through the TCA.

Limitations

Although our results provide a comprehensive view of genomic, proteomic, and metabolic changes associated with an increase in the myocardial levels of histidyl dipeptides, the study has several limitation. First, we used a transgenesis approach to study the effect of histidyl dipeptides on cardiac structure, gene expression, and metabolism. These changes were attributable to a 20- to 25-fold increase in the levels of histidyl dipeptides in the heart. We previously reported that β-alanine feeding for 7 days only enhances myocardial carnosine levels 7- to 10-fold,[18] suggesting that the increase in myocardial histidyl dipeptides by transgenesis is similar in magnitude than could be achieved physiologically by prolonged β-alanine feeding. Second, even though our studies reveal the widespread impact of increased histidyl dipeptides, which could be achieved under physiological conditions, previous work has shown that carnosine levels are depleted in the skeletal muscle of patients with type 2 diabetes,[66] patients of older age,[67] and patients with chronic obstructive pulmonary diseases.[68] How depletion of carnosine, as opposed to an increase, could affect the proteome/genome/metabolome of the heart remains unknown and requires additional studies on mice with low levels of carnosine caused by pathophysiological changes or deletion of the Carns gene.

Finally, in the present study we overexpressed *Carns* in cardiomyocytes, used the whole heart to analyze the effects of this overexpression, and did not examine the effect of increased histidyl dipeptides on other cells, such as fibroblasts and endothelial cells. Given that exogenous expression of *Carns* was driven by the α-MHC promoter, which is highly specific for cardiomyocytes, it seems unlikely that the levels of

histidyl dipeptides were increased in non–MHC-containing cells in the heart or other tissues. Moreover, even though the levels of histidyl dipeptides were enhanced manifold in the CarnsTg hearts, no changes were observed in the circulating levels of histidyl dipeptides (results not shown), suggesting that these dipeptides are not extruded out from the cardiomyocytes to alter histidyl dipeptides in distal tissue. Nonetheless, additional measurements in cells other than cardiac myocytes are needed to determine whether altering histidyl dipeptides in the cardiomyocytes affects levels of histidyl dipeptides or other proteins in fibroblasts and endothelial cells of the heart.

Multiomics Approach Elucidates the Impact of Histidyl Dipeptides

Overall, in this study, by using a well-defined model of a single gene overexpression, localized to the heart, we were able to identify multiple transcriptomic, proteomic, and metabolomic changes in the heart. Many of the proteomic changes were concordant with the changes in metabolism and with the overall metabolic protection provided by histidyl dipeptides to the ischemic heart. During the course of this work, we identified several previously unknown changes in metabolites, transcripts, and proteins, presumably triggered by increasing the levels of histidyl dipeptides in the heart, and determined how these changes act in concert to create a metabolic milieu that resists ischemic injury. To our knowledge, this is the first study to use the system biology approach to identify the metabolic, molecular, and cellular pathways in ischemic and nonischemic hearts and how they are affected by increasing the synthesis of histidyl dipeptides in the heart. Of importance, multiomics integration of the data revealed potential parallels at the genome, proteome, and metabolome levels in the heart, showing that the well-established FA metabolism and TCA, enriched at the miRNA and protein levels, overlap with the enrichment of FA oxidation and TCA metabolites. The unbiased assessment of metabolic changes in the ischemic heart, and the findings that ischemic accumulation of FFA was attenuated in CarnsTg hearts reveals novel insights into the reprogramming at the gene and protein levels, which impacts both β-oxidation and glycolysis. Our findings show that a combinatorial effect of these dipeptides on multiple pathways, particularly FA and glucose utilization, could potentially contribute to optimizing the use of cardiac fuels under physiological and pathological conditions to impart a pervasive protection against ischemic injury. Given that the histidyl dipeptides in heart and muscle could be increased under physiological conditions such as β-alanine feeding and exercise,[18,14] our findings provide a new understanding of the mechanisms underlying the cardioprotective effects of histidyl dipeptides. Finally, because myocardial levels of histidyl dipeptides could be readily increased by feeding carnosine or β-alanine, these results also suggest a readily adaptable intervention to improve basal metabolism in the heart and to increase myocardial resistance to ischemic injury.

ARTICLE INFORMATION

Received September 24, 2021; accepted April 21, 2022.

Affiliations

Beijing Institute of Genomics, Chinese Academy of Sciences, Beishan Industrial Zone, Shenzhen, China (K.Y., Z.M., S.L.), Diabetes and Obesity Center (J.Z., K.K., B.D., D.H., D.K.P., P.K.L., A.B., S.P.B.), Christina Lee Brown Envirome Institute (J.Z., K.K., B.D., D.H., D.K.P., P.K.L., A.B., S.P.B.), and Department of Chemistry (M.A.I.P., L.H., X.Y., X.Z.), University of Louisville, KY; Department of Anesthesiology and Perioperative and Pain Medicine, Stanford University, Palo Alto, CA (D.O.); Department of Medicine, Medical college, The Aga Khan University, Nairobi, Kenya (J.S.); and Biostatistics Shared Facility, University of Louisville Health, Brown Cancer Center, Louisville, KY (J.P., S.R.).

Acknowledgments

We thank D. Mosley, F. Li, and the Diabetes and Obesity Center's Imaging and Physiological Core and Animal Models and Phenotyping Core at the University of Louisville for technical assistance.

Sources of Funding

This work was supported by the National Institutes of Health (R01HL122581–01 [Baba], R01HL 55 477, GM127607 [Bhatnagar]) and the Jewish Heritage Fund for Excellence (GN210596F).

Disclosures

None.

Supplemental Material

Data S1–S5
Figures S1–S7

REFERENCES

1. Drozak J, Veiga-da-Cunha M, Vertommen D, Stroobant V, Van Schaftingen E. Molecular identification of carnosine synthase as ATP-grasp domain-containing protein 1 (ATPGD1). *J Biol Chem*. 2010;285:9346–9356. doi: 10.1074/jbc.M109.095505
2. Boldyrev AA, Aldini G, Derave W. Physiology and pathophysiology of carnosine. *Physiol Rev*. 2013;93:1803–1845. doi: 10.1152/physrev.00039.2012
3. Abe H. Role of histidine-related compounds as intracellular proton buffering constituents in vertebrate muscle. *Biochemistry (Mosc)*. 2000;65:757–765.
4. Aldini G, Carini M, Beretta G, Bradamante S, Facino RM. Carnosine is a quencher of 4-hydroxy-nonenal: through what mechanism of reaction? *Biochem Biophys Res Commun*. 2002;298:699–706. doi: 10.1016/S0006-291X(02)02545-7
5. Baba SP, Hoetker JD, Merchant M, Klein JB, Cai J, Barski OA, Conklin DJ, Bhatnagar A. Role of aldose reductase in the metabolism and detoxification of carnosine-acrolein conjugates. *J Biol Chem*. 2013;288:28163–28179. doi: 10.1074/jbc.M113.504753
6. Zhao J, Posa DK, Kumar V, Hoetker D, Kumar A, Ganesan S, Riggs DW, Bhatnagar A, Wempe MF, Baba SP. Carnosine protects cardiac myocytes against lipid peroxidation products. *Amino Acids*. 2019;51:123–138. doi: 10.1007/s00726-018-2676-6
7. Ihara H, Kakihana Y, Yamakage A, Kai K, Shibata T, Nishida M, Yamada KI, Uchida K. 2-Oxo-histidine-containing dipeptides are functional oxidation products. *J Biol Chem*. 2019;294:1279–1289. doi: 10.1074/jbc.RA118.006111
8. Letzien U, Oppermann H, Meixensberger J, Gaunitz F. The antineoplastic effect of carnosine is accompanied by induction of PDK4 and can be mimicked by L-histidine. *Amino Acids*. 2014;46:1009–1019. doi: 10.1007/s00726-014-1664-8

9. Ito-Kato E, Suzuki N, Maeno M, Takada T, Tanabe N, Takayama T, Ito K, Otsuka K. Effect of carnosine on runt-related transcription factor-2/core binding factor alpha-1 and Sox9 expressions of human periodontal ligament cells. *J Periodontal Res*. 2004;39:199–204. doi: 10.1111/j.1600-0765.2004.00725.x
10. Sugihara Y, Onoue S, Tashiro K, Sato M, Hasegawa T, Katakura Y. Carnosine induces intestinal cells to secrete exosomes that activate neuronal cells. *PLoS One*. 2019;14:e0217394. doi: 10.1371/journal.pone.0217394
11. Iovine B, Oliviero G, Garofalo M, Orefice M, Nocella F, Borbone N, Piccialli V, Centore R, Mazzone M, Piccialli G, et al. The anti-proliferative effect of L-carnosine correlates with a decreased expression of hypoxia inducible factor 1 alpha in human colon cancer cells. *PLoS One*. 2014;9:e96755. doi: 10.1371/journal.pone.0096755
12. Zhang Z, Miao L, Wu X, Liu G, Peng Y, Xin X, Jiao B, Kong X. Carnosine inhibits the proliferation of human gastric carcinoma cells by retarding Akt/mTOR/p70S6K signaling. *J Cancer*. 2014;5:382–389. doi: 10.7150/jca.8024
13. Wang JP, Yang ZT, Liu C, He YH, Zhao SS. L-carnosine inhibits neuronal cell apoptosis through signal transducer and activator of transcription 3 signaling pathway after acute focal cerebral ischemia. *Brain Res*. 2013;1507:125–133. doi: 10.1016/j.brainres.2013.02.032
14. Hoetker D, Chung W, Zhang D, Zhao J, Schmidtke VK, Riggs DW, Derave W, Bhatnagar A, Bishop DJ, Baba SP. Exercise alters and beta-alanine combined with exercise augments histidyl dipeptide levels and scavenges lipid peroxidation products in human skeletal muscle. *J Appl Physiol (1985)*. 2018;125:1767–1778. doi: 10.1152/japplphysiol.00007.2018
15. Schnuck JK, Sunderland KL, Kuennen MR, Vaughan RA. Characterization of the metabolic effect of beta-alanine on markers of oxidative metabolism and mitochondrial biogenesis in skeletal muscle. *J Exerc Nutrition Biochem*. 2016;20:34–41. doi: 10.20463/jenb.2016.06.20.2.5
16. Sansbury BE, DeMartino AM, Xie Z, Brooks AC, Brainard RE, Watson LJ, DeFilippis AP, Cummins TD, Harbeson MA, Brittian KR, et al. Metabolomic analysis of pressure-overloaded and infarcted mouse hearts. *Circ Heart Fail*. 2014;7:634–642. doi: 10.1161/CIRCHEARTFAILURE.114.001151
17. Lee JW, Miyawaki H, Bobst EV, Hester JD, Ashraf M, Bobst AM. Improved functional recovery of ischemic rat hearts due to singlet oxygen scavengers histidine and carnosine. *J Mol Cell Cardiol*. 1999;31:113–121. doi: 10.1006/jmcc.1998.0850
18. Zhao J, Conklin DJ, Guo Y, Zhang X, Obal D, Guo L, Jagatheesan G, Katragadda K, He L, Yin X, et al. Cardiospecific overexpression of ATPGD1 (carnosine synthase) increases histidine dipeptide levels and prevents myocardial ischemia reperfusion injury. *J Am Heart Assoc*. 2020;9:e015222. doi: 10.1161/JAHA.119.015222
19. Gillet LC, Navarro P, Tate S, Rost H, Selevsek N, Reiter L, Bonner R, Aebersold R. Targeted data extraction of the MS/MS spectra generated by data-independent acquisition: a new concept for consistent and accurate proteome analysis. *Mol Cell Proteomics*. 2012;11:O111.016717.
20. Anjo SI, Santa C, Manadas B. SWATH-MS as a tool for biomarker discovery: from basic research to clinical applications. *Proteomics*. 2017;17:1–23.
21. Dorus S, Busby SA, Gerike U, Shabanowitz J, Hunt DF, Karr TL. Genomic and functional evolution of the *Drosophila melanogaster* sperm proteome. *Nat Genet*. 2006;38:1440–1445. doi: 10.1038/ng1915
22. Vizcaino JA, Deutsch EW, Wang R, Csordas A, Reisinger F, Rios D, Dianes JA, Sun Z, Farrah T, Bandeira N, et al. ProteomeXchange provides globally coordinated proteomics data submission and dissemination. *Nat Biotechnol*. 2014;32:223–226. doi: 10.1038/nbt.2839
23. Liu W, Wang X. Prediction of functional microRNA targets by integrative modeling of microRNA binding and target expression data. *Genome Biol*. 2019;20:18. doi: 10.1186/s13059-019-1629-z
24. Koo I, Shi X, Kim S, Zhang X. iMatch2: compound identification using retention index for analysis of gas chromatography-mass spectrometry data. *J Chromatogr A*. 2014;1337:202–210. doi: 10.1016/j.chroma.2014.02.049
25. Wei X, Shi X, Koo I, Kim S, Schmidt RH, Arteel GE, Watson WH, McClain C, Zhang X. MetPP: a computational platform for comprehensive two-dimensional gas chromatography time-of-flight mass spectrometry-based metabolomics. *Bioinformatics*. 2013;29:1786–1792. doi: 10.1093/bioinformatics/btt275
26. Zhang J, Fang A, Wang B, Kim SH, Bogdanov B, Zhou Z, McClain C, Zhang X. iMatch: a retention index tool for analysis of gas chromatography–mass spectrometry data. *J Chromatogr A*. 2011;1218:6522–6530. doi: 10.1016/j.chroma.2011.07.039
27. Tarazona S, Garcia-Alcalde F, Dopazo J, Ferrer A, Conesa A. Differential expression in RNA-seq: a matter of depth. *Genome Res*. 2011;21:2213–2223. doi: 10.1101/gr.124321.111
28. Raju TN. William Sealy Gosset and William A. Silverman: two "students" of science. *Pediatrics*. 2005;116:732–735. doi: 10.1542/peds.2005-1134
29. Goh WW, Lee YH, Chung M, Wong L. How advancement in biological network analysis methods empowers proteomics. *Proteomics*. 2012;12:550–563. doi: 10.1002/pmic.201100321
30. Greenbaum D, Jansen R, Gerstein M. Analysis of mRNA expression and protein abundance data: an approach for the comparison of the enrichment of features in the cellular population of proteins and transcripts. *Bioinformatics*. 2002;18:585–596. doi: 10.1093/bioinformatics/18.4.585
31. Zhang W, Culley DE, Scholten JC, Hogan M, Vitiritti L, Brockman FJ. Global transcriptomic analysis of *Desulfovibrio vulgaris* on different electron donors. *Antonie Van Leeuwenhoek*. 2006;89:221–237. doi: 10.1007/s10482-005-9024-z
32. Nie L, Wu G, Culley DE, Scholten JC, Zhang W. Integrative analysis of transcriptomic and proteomic data: challenges, solutions and applications. *Crit Rev Biotechnol*. 2007;27:63–75. doi: 10.1080/07388550701334212
33. Crick F. Central dogma of molecular biology. *Nature*. 1970;227:561–563. doi: 10.1038/227561a0
34. Gygi SP, Rochon Y, Franza BR, Aebersold R. Correlation between protein and mRNA abundance in yeast. *Mol Cell Biol*. 1999;19:1720–1730. doi: 10.1128/MCB.19.3.1720
35. Heer KR, Stalder H, Thoelen H. Early appearance of 2,3-butanediol in acute myocardial infarction. A new marker for ischaemia? *Eur Heart J*. 1990;11:788–790. doi: 10.1093/oxfordjournals.eurheartj.a059798
36. Heer KR, Althaus U, Mettler D, Schilt W, Thoelen H. 2,3-butanediol in experimental myocardial ischaemia in pigs. *Eur Heart J*. 1991;12:654–656. doi: 10.1093/oxfordjournals.eurheartj.a059956
37. Vadaszova A, Zacharova G, Machacova K, Jirmanova I, Soukup T. Influence of thyroid status on the differentiation of slow and fast muscle phenotypes. *Physiol Res*. 2004;53(suppl 1):S57–S61.
38. Clark KL, Yutzey KE, Benson DW. Transcription factors and congenital heart defects. *Annu Rev Physiol*. 2006;68:97–121. doi: 10.1146/annurev.physiol.68.040104.113828
39. van Rooij E, Quiat D, Johnson BA, Sutherland LB, Qi X, Richardson JA, Kelm RJ Jr, Olson EN. A family of microRNAs encoded by myosin genes governs myosin expression and muscle performance. *Dev Cell*. 2009;17:662–673. doi: 10.1016/j.devcel.2009.10.013
40. Morano I, Hadicke K, Grom S, Koch A, Schwinger RH, Bohm M, Bartel S, Erdmann E, Krause EG. Titin, myosin light chains and C-protein in the developing and failing human heart. *J Mol Cell Cardiol*. 1994;26:361–368. doi: 10.1006/jmcc.1994.1045
41. Tsukamoto O, Kitakaze M. Biochemical and physiological regulation of cardiac myocyte contraction by cardiac-specific myosin light chain kinase. *Circ J*. 2013;77:2218–2225.
42. Yin K, Ma Y, Cui H, Sun Y, Han B, Liu X, Zhao K, Li W, Wang J, Wang H, et al. The co-segregation of the MYL2 R58Q mutation in Chinese hypertrophic cardiomyopathy family and its pathological effect on cardiomyopathy disarray. *Mol Genet Genomics*. 2019;294:1241–1249. doi: 10.1007/s00438-019-01578-4
43. Chouchani ET, Pell VR, Gaude E, Aksentijevic D, Sundier SY, Robb EL, Logan A, Nadtochiy SM, Ord ENJ, Smith AC, et al. Ischaemic accumulation of succinate controls reperfusion injury through mitochondrial ROS. *Nature*. 2014;515:431–435. doi: 10.1038/nature13909
44. Lopaschuk GD, Ussher JR, Folmes CD, Jaswal JS, Stanley WC. Myocardial fatty acid metabolism in health and disease. *Physiol Rev*. 2010;90:207–258. doi: 10.1152/physrev.00015.2009
45. Weisiger RA. Cytosolic fatty acid binding proteins catalyze two distinct steps in intracellular transport of their ligands. *Mol Cell Biochem*. 2002;239:35–43. doi: 10.1023/A:1020550405578
46. Jaswal JS, Keung W, Wang W, Ussher JR, Lopaschuk GD. Targeting fatty acid and carbohydrate oxidation—a novel therapeutic intervention in the ischemic and failing heart. *Biochim Biophys Acta*. 2011;1813:1333–1350. doi: 10.1016/j.bbamcr.2011.01.015
47. Warren JS, Oka SI, Zablocki D, Sadoshima J. Metabolic reprogramming via PPARalpha signaling in cardiac hypertrophy and failure: from metabolomics to epigenetics. *Am J Physiol Heart Circ Physiol*. 2017;313:H584–H596. doi: 10.1152/ajpheart.00103.2017

48. Neely JR, Morgan HE. Relationship between carbohydrate and lipid metabolism and the energy balance of heart muscle. *Annu Rev Physiol*. 1974;36:413–459. doi: 10.1146/annurev.ph.36.030174.002213
49. Lloyd SG, Wang P, Zeng H, Chatham JC. Impact of low-flow ischemia on substrate oxidation and glycolysis in the isolated perfused rat heart. *Am J Physiol Heart Circ Physiol*. 2004;287:H351–H362. doi: 10.1152/ajpheart.00983.2003
50. Whitmer JT, Idell-Wenger JA, Rovetto MJ, Neely JR. Control of fatty acid metabolism in ischemic and hypoxic hearts. *J Biol Chem*. 1978;253:4305–4309. doi: 10.1016/S0021-9258(17)34720-8
51. Bergmann SR. Cardiac positron emission tomography. *Semin Nucl Med*. 1998;28:320–340. doi: 10.1016/S0001-2998(98)80036-6
52. Vetter NJ, Strange RC, Adams W, Oliver MF. Initial metabolic and hormonal response to acute myocardial infarction. *Lancet*. 1974;1:284–288. doi: 10.1016/S0140-6736(74)92595-1
53. Raz A, Livne A. Differential effects of lipids on the osmotic fragility of erythrocytes. *Biochim Biophys Acta*. 1973;311:222–229. doi: 10.1016/0005-2736(73)90269-1
54. Adams RJ, Cohen DW, Gupte S, Johnson JD, Wallick ET, Wang T, Schwartz A. In vitro effects of palmitylcarnitine on cardiac plasma membrane Na,K-ATPase, and sarcoplasmic reticulum Ca^{2+}-ATPase and Ca^{2+} transport. *J Biol Chem*. 1979;254:12404–12410. doi: 10.1016/S0021-9258(19)86329-9
55. Dhalla NS, Kolar F, Shah KR, Ferrari R. Effects of some L-carnitine derivatives on heart membrane ATPases. *Cardiovasc Drugs Ther*. 1991;5(suppl 1):25–30. doi: 10.1007/BF00128240
56. Lopaschuk GD, Wall SR, Olley PM, Davies NJ. Etomoxir, a carnitine palmitoyltransferase I inhibitor, protects hearts from fatty acid-induced ischemic injury independent of changes in long chain acylcarnitine. *Circ Res*. 1988;63:1036–1043. doi: 10.1161/01.RES.63.6.1036
57. Lopaschuk GD, Spafford MA, Davies NJ, Wall SR. Glucose and palmitate oxidation in isolated working rat hearts reperfused after a period of transient global ischemia. *Circ Res*. 1990;66:546–553. doi: 10.1161/01.RES.66.2.546
58. Lopaschuk GD, McNeil GF, McVeigh JJ. Glucose oxidation is stimulated in reperfused ischemic hearts with the carnitine palmitoyltransferase 1 inhibitor, Etomoxir. *Mol Cell Biochem*. 1989;88:175–179.
59. Coort SL, Willems J, Coumans WA, van der Vusse GJ, Bonen A, Glatz JF, Luiken JJ. Sulfo-N-succinimidyl esters of long chain fatty acids specifically inhibit fatty acid translocase (FAT/CD36)-mediated cellular fatty acid uptake. *Mol Cell Biochem*. 2002;239:213–219. doi: 10.1023/A:1020539932353
60. Lopaschuk GD, Folmes CD, Stanley WC. Cardiac energy metabolism in obesity. *Circ Res*. 2007;101:335–347. doi: 10.1161/CIRCRESAHA.107.150417
61. Finck BN, Han X, Courtois M, Aimond F, Nerbonne JM, Kovacs A, Gross RW, Kelly DP. A critical role for PPARalpha-mediated lipotoxicity in the pathogenesis of diabetic cardiomyopathy: modulation by dietary fat content. *Proc Natl Acad Sci USA*. 2003;100:1226–1231. doi: 10.1073/pnas.0336724100
62. McGarry JD, Dobbins RL. Fatty acids, lipotoxicity and insulin secretion. *Diabetologia*. 1999;42:128–138. doi: 10.1007/s001250051130
63. Unger RH. Minireview: weapons of lean body mass destruction: the role of ectopic lipids in the metabolic syndrome. *Endocrinology*. 2003;144:5159–5165. doi: 10.1210/en.2003-0870
64. Yagyu H, Chen G, Yokoyama M, Hirata K, Augustus A, Kako Y, Seo T, Hu Y, Lutz EP, Merkel M, et al. Lipoprotein lipase (LpL) on the surface of cardiomyocytes increases lipid uptake and produces a cardiomyopathy. *J Clin Invest*. 2003;111:419–426. doi: 10.1172/JCI16751
65. Ashrafian H, Czibik G, Bellahcene M, Aksentijevic D, Smith AC, Mitchell SJ, Dodd MS, Kirwan J, Byrne JJ, Ludwig C, et al. Fumarate is cardioprotective via activation of the Nrf2 antioxidant pathway. *Cell Metab*. 2012;15:361–371. doi: 10.1016/j.cmet.2012.01.017
66. Gualano B, Everaert I, Stegen S, Artioli GG, Taes Y, Roschel H, Achten E, Otaduy MC, Junior AH, Harris R, et al. Reduced muscle carnosine content in type 2, but not in type 1 diabetic patients. *Amino Acids*. 2012;43:21–24. doi: 10.1007/s00726-011-1165-y
67. Krumpolec P, Klepochova R, Just I, Tusek Jelenc M, Frollo I, Ukropec J, Ukropcova B, Trattnig S, Krssak M, Valkovic L. Multinuclear MRS at 7T uncovers exercise driven differences in skeletal muscle energy metabolism between young and seniors. *Front Physiol*. 2020;11:644. doi: 10.3389/fphys.2020.00644
68. De Brandt J, Burtin C, Pomies P, Vandenabeele F, Verboven K, Aumann J, Blancquaert L, Everaert I, Van Ryckeghem L, Cops J, et al. Carnosine, oxidative and carbonyl stress, antioxidants, and muscle fiber characteristics of quadriceps muscle of patients with COPD. *J Appl Physiol (1985)*. 2021;131:1230–1240. doi: 10.1152/japplphysiol.00200.2021

SUPPLEMENTAL MATERIAL

Data S1. Differentially regulated coding and non-coding genes in the carnosine synthase transgenic (CarnsTg) heart.

Data S2. Differentially expressed proteins in the carnosine synthase transgenic (CarnsTg) heart.

Data S3. Metabolites altered in the carnosine synthase transgenic (CarnsTg) heart under basal conditions detected by MTBSTFA derivatization.

Data S4. Metabolites altered in the carnosine synthase transgenic (CarnsTg) heart under basal conditions detected by MSTFA derivatization.

Data S5. Significantly altered metabolites in wild type heart and carnosine synthase transgenic (CarnsTg)Data S1 hearts that were subjected to 35 min of perfusion followed by 5- and 15-min ischemia.

Figure S1. Levels of histidyl dipeptides in the wild type (WT) and carnosine synthase transgenic (CarnsTg) mice.

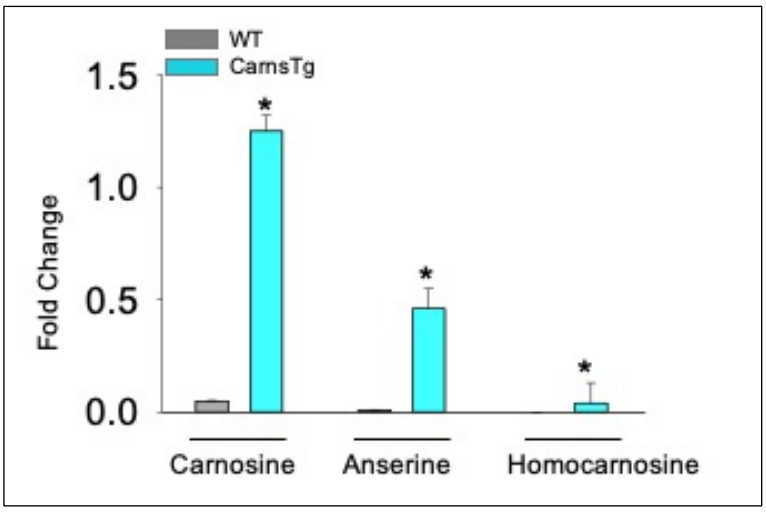

Hearts from the WT and CarnsTg mice were isolated and analyzed for histidyl dipeptides carnosine, anserine, homocarnosine and carcinine using LC/MS/MS methods and ^{4}d carnosine and tyrosyl-histidine as internal standard. Chromatograms were acquired using the transitions carnosine 227→110 *m/z*, homocarnosine 241→156 *m/z*, anserine 241→109 *m/z* and carcinine 182→110 *m/z*. Data are presented as mean±SEM, n=4 samples in each group.

Figure S2: **Comparative analysis of the differentially expressed proteins (DEPs) between the wild type (WT) and carnosine synthase transgenic (CarnsTg) hearts**.

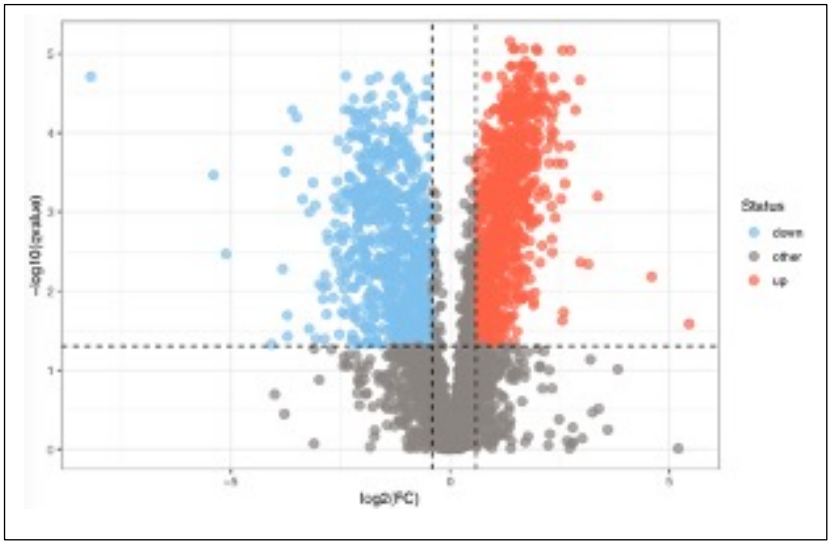

Volcano plot of the proteome between the WT and CarnsTg hearts, where the statistical significance $\log_{10}$ of *p*-value Y-axis was plotted against $\log_2$-fold change (X-axis).

Figure S3: Metabolomic analysis of the wild type (WT) and carnosine synthase transgenic (CarnsTg) hearts under basal conditions.

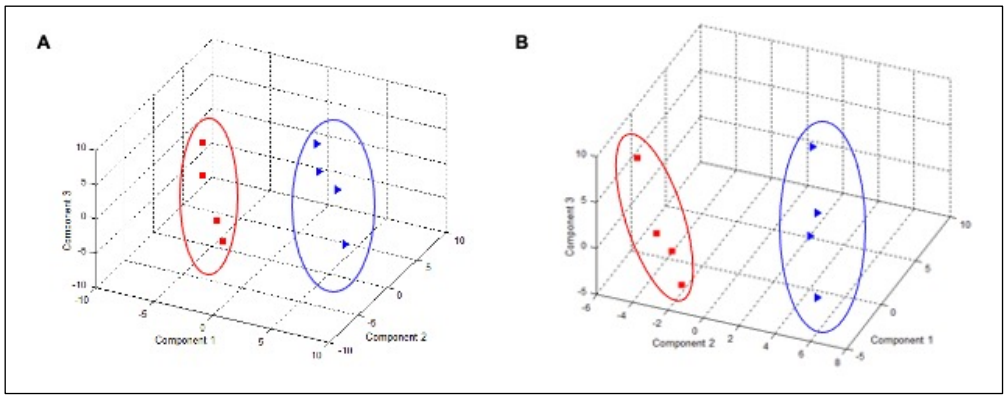

Changes in the global cardio metabolomic profile by Carns overexpression were assessed using an unbiased metabolomic approach. Partial least square plot (PLS-DA) of the metabolites from the WT and CarnsTg mice hearts under basal conditions detected by (**A**) MTBSTFA and (**B**) MSTFA derivatization.

Figure S4: Non-targeted metabolomic analysis of the wild type (WT) and carnosine synthase transgenic (CarnsTg) perfused mice hearts.

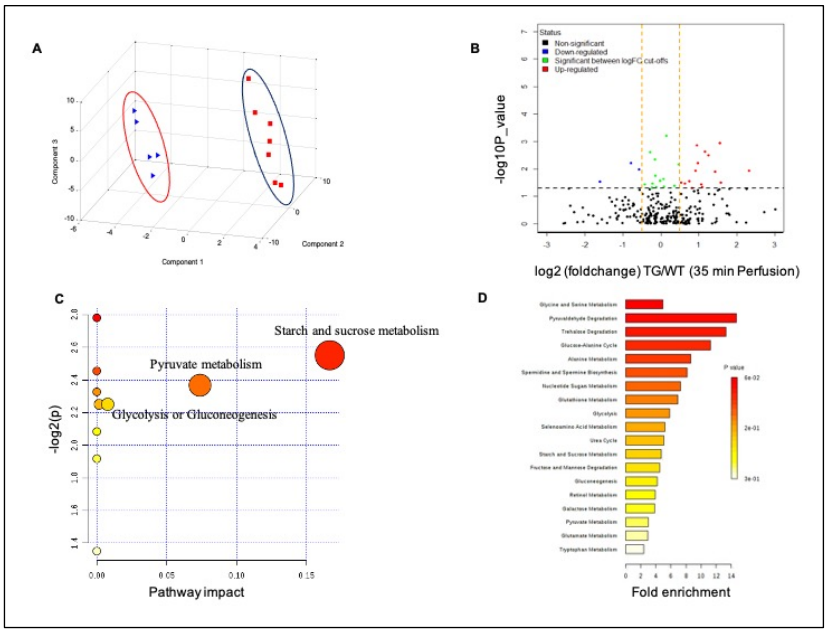

Isolated hearts from the WT and CarnsTg mice were perfused in a Langendorff mode for 35 min. (**A**) principal component analysis, (**B**) Volcano plot, (**C**) pathway impact analysis and (**D**) enrichment analysis of metabolic sets modulated by Carns overexpression relative to WT, n=7 in each group.

Figure S5: Metabolomic analysis of the wild type (WT) and carnosine synthase transgenic (Carns Tg) hearts during different durations of ischemia.

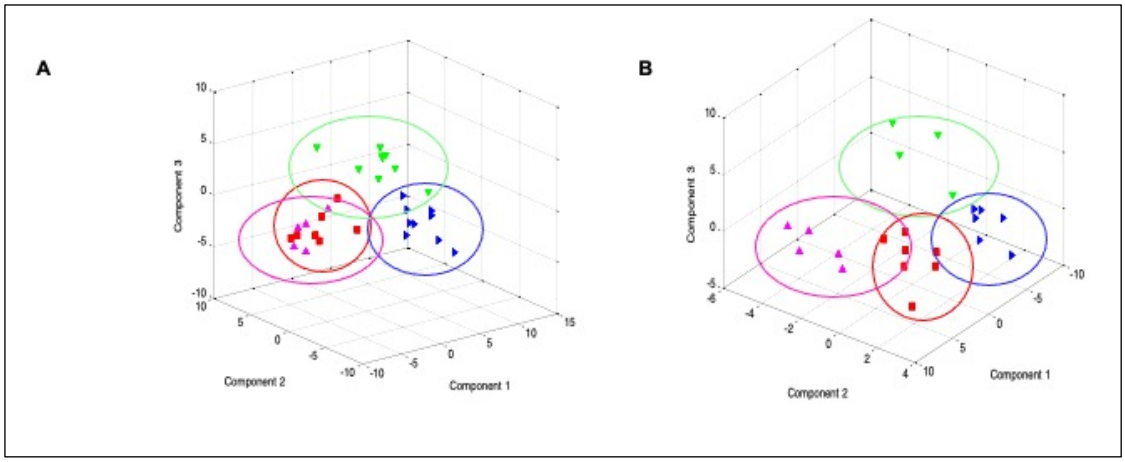

PLS-DA of the WT and CarnsTg hearts following (**E**) 5 min and (**F**) 15 min of ischemia, where purple symbol represents metabolites from the WT heart subjected to 35 min perfusion, red symbol represents metabolites from CarnsTg heart perfused for 35 min, green symbols represent metabolites from WT heart subjected to 20 min perfusion followed by 5 min ischemia, blue symbols represent metabolites from CarnsTg heart perfused for 20 min followed by 15 min ischemia.

Figure S6. Impact analysis shows the effect of ischemia on the primary metabolic pathway.

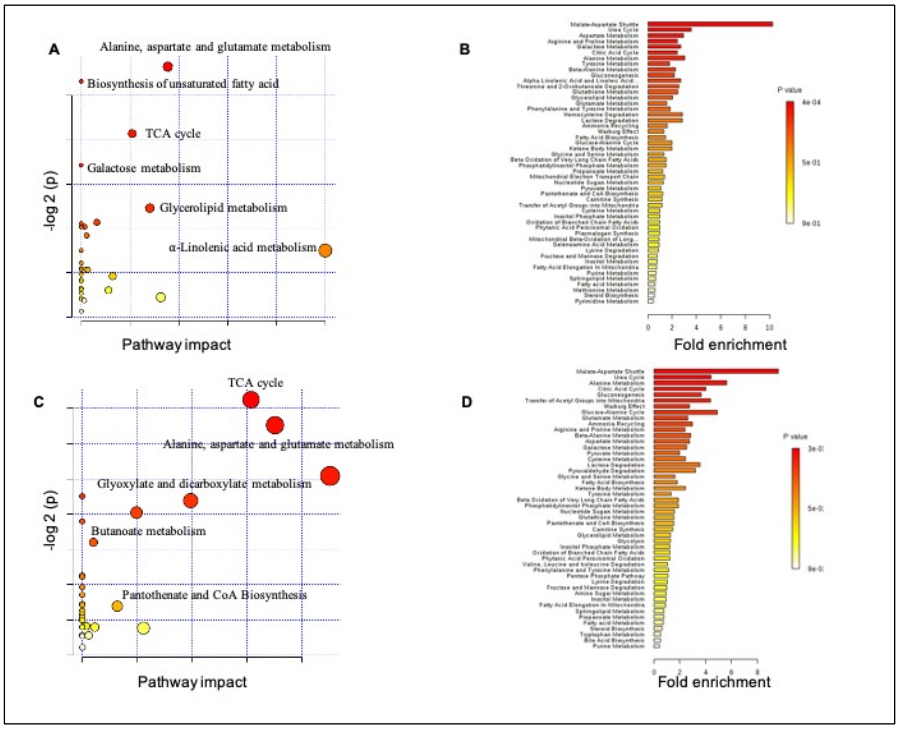

Impact analysis induced by (**A**) 5 min and (**C**) 15 min of ischemia in the wild type (WT) mice hearts. Enrichment analysis of metabolic sets modulated after (**C**) 5 min and (**D**) 15 min of ischemia in the WT hearts, n=7 in each group.

Figure S7. Carnosine synthase (Carns) overexpression in heart affects the expression of different cytosolic and mitochondrial proteins.

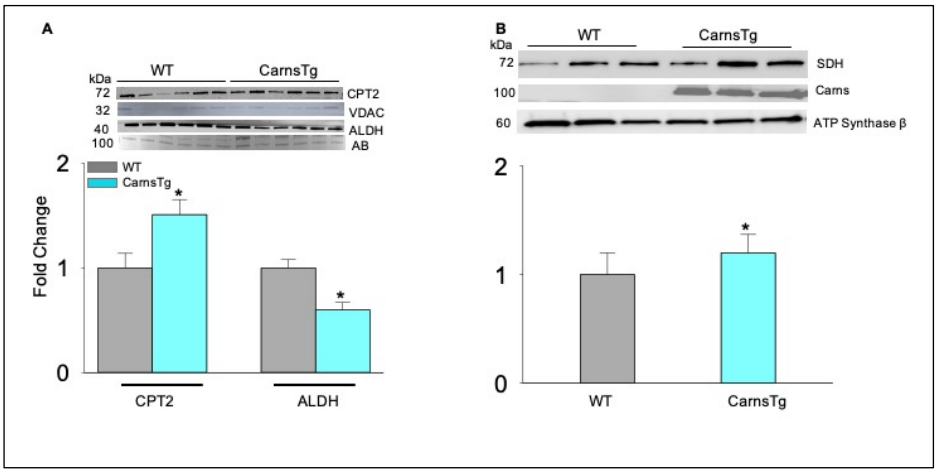

(A) Western blot analysis of the carnitine palmitoyl transferase 2 (CPT2) in the mitochondria, and aldehyde dehydrogenase (ALDH) in the cytosol of the wild type (WT) and CarnsTg hearts. Succinate dehydrogenase (SDH) expression in the mitochondrial fraction, and Carns expression in the cytosol of the WT and Carns transgenic mice hearts. Data presented as fold change is normalized to voltage dependent ion channel (VDAC), ATP synthase β and amido black, *$p<0.05$ vs WT, n=4-6 samples in each group**.**